

Photonics Modeling and Fabrication at Sandia National Laboratories

**David W. Peters, S. A. Kemme, G. R. Hadley, J. R.
Wendt, T. R. Carter, S. Samora, I. F. El-Kady**

**Applied Photonic Microsystems
Sandia National Laboratories**

**dwpeter@sandia.gov
(505) 845-9244**



Outline

- **Sandia's background, mission, and capabilities**
- **Resonant Subwavelength Gratings**
- **Surface Plasmon Modeling**
- **Photonic Crystal Modeling**



Sandia National Laboratories



California

New Mexico



- Rich History: Part of Z-Division (LANL) in Manhattan Project; created as Nation's "Engineering Arm" in 1949 by President Truman
- Today 8,000 employees in New Mexico, California, Nevada, and Hawaii
- Responsible for research, development, engineering, and maintenance of U.S. nuclear weapons
- Responsible for all non-nuclear subsystems; the primary systems integration and engineering lab
- \$2B annual budget
- \$550M from other federal agencies
- \$50M from private industry through R&D partnerships

"Helping our nation secure a peaceful and free world through technology"



Sandia National Laboratories

7000 full time employees
~6000 in New Mexico
~1000 in California

600 buildings, 5M square feet



1400 Ph.D.'s, 1700 Masters
55% engineering
33% science & mathematics
12% computing





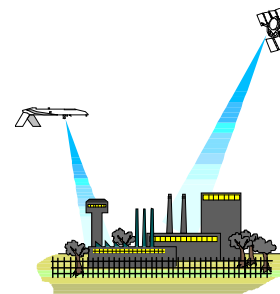
Sandia is Organized into 4 Strategic Management Units (SMUs) and 1 Initiative

Military Technologies and Applications

Advanced Technology to Protect the Nation



Non-Proliferation & Assessments



Surveillance

Detection

Energy & Infrastructure Assurance



Energy

Information

Nuclear Weapons



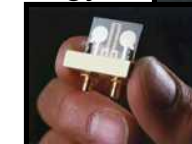
Safe, Secure, Reliable Weapons

Homeland Security Initiative



Architectural Surety

Anti-crime and anti-terrorism technology

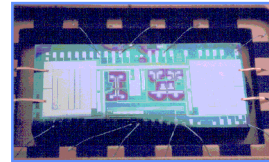


Smart Weapons

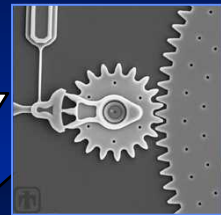
Transportation

Sandia's Enabling Capabilities Produce Miniature Sensors, Processors, and Communication Systems

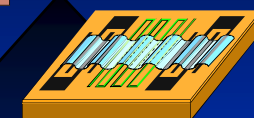
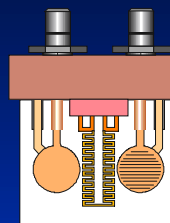
Sense, Process, Communicate



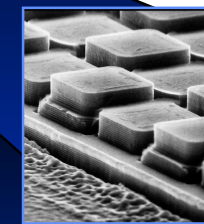
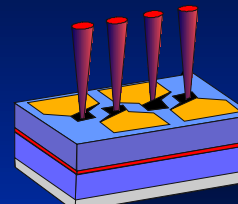
**Micromachines,
Microelectronics**



Micsensors



**Photonics,
Microwave Circuits**

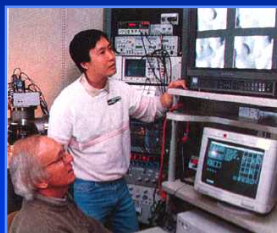


**Microelectronics
Development Laboratory
MDL**



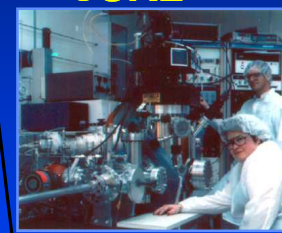
Over 30,000 ft² of
clean room, Class 1 μ E
Fabrication Facility

**Integrated Materials
Research Laboratory
IMRL**

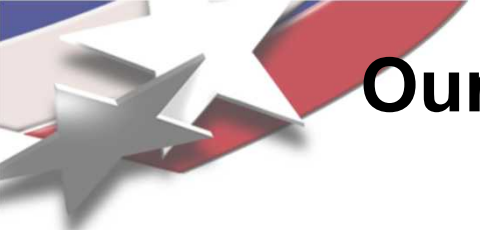


Materials Fabrication and
Characterization, including Plasma
Deposition and Surface and
Interface State Characterization

**Compound Semiconductor
Research Laboratory
CSRL**



MOCVD, MBE Deposition,
Electron Beam Lithography,
Reactive Ion Beam Etching
National
laboratories



Our Mission Requires Unique and Distinguishing Facilities



Integrated Materials
Research Laboratory



Integrated Manufacturing
Technologies Laboratory
Complex (IMTL)



Microsystem and
Engineering
Science Applications
(MESA) Facility



Compound
Semiconductor
Research Laboratory
(CSRL)



Microelectronics
Development
Lab (MDL)



Processing and
Environmental
Technology Laboratory
(PETL)



Science, and Engineering
Laboratory (RMSEL)



Microsystems Science, Technology & Components

Microelectronic Development Laboratory (MDL)

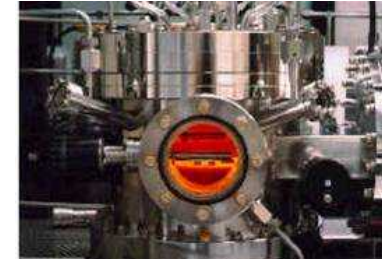
- Over 30,000 Square Feet of Clean Room Space
- State-of-the-art equipment for processing wafers up to 6 inches in Diameter
- 22 Separate laminar flow clean room bays- each with an independent air supply
- The Multiple clean room bays collectively provide over 12,000 square feet of class 1 clean room space.
(Less than 1 particle 0.5 micron or larger per cubic foot of air.)



Compound Semiconductor Research Laboratory (CSRL)

6500-square-foot (net) class 100 Clean Room Supports:

- Microsystem Skunkwork
- (Compound) Semiconductor Materials Growth and Processing
- RF & Photonic Device Technologies
- Microsensors Fabrication
- Hybrid Integration/Advanced Packaging



Mesa Complex

Components



System Engineering



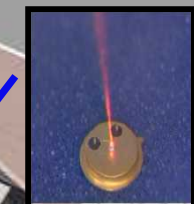
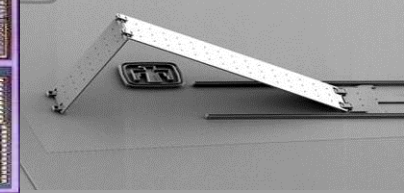
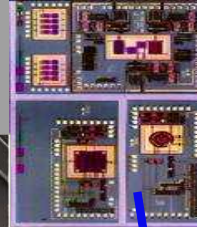
MESA Provides Top Facilities and Equipment For Microsystems Design, Fabrication and Test
Complete: FY06

Construction: \$77M
Equipment: \$16M

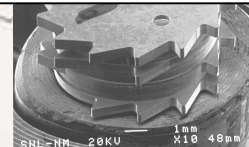


TOTALS: Construction: \$246M, Equipment: \$168M
Contingency: \$49M, TEC: \$463M

Construction: \$114M
Equipment: \$139M



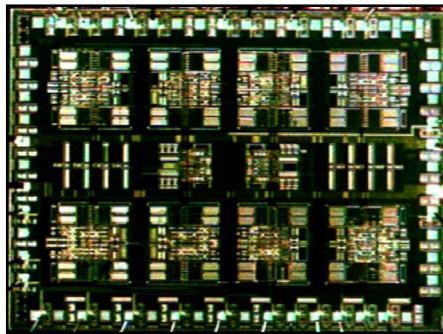
Science



Construction: \$55M
Equipment: \$13M

Microelectronics Technologies

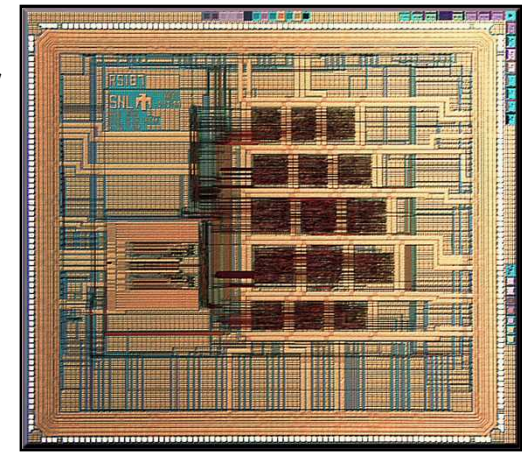
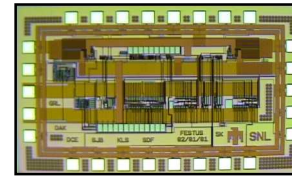
Analog, Bipolar IC for 256-Channel Gamma Spectrometer



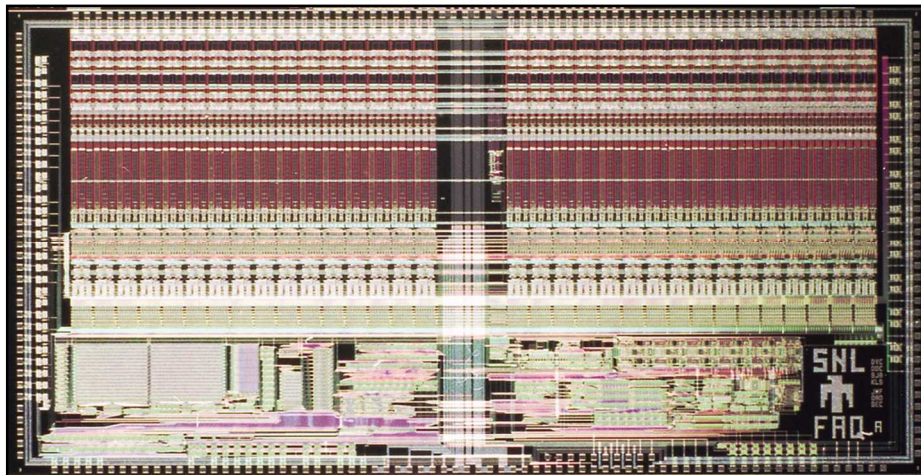
Charge Amp / Shaping Amp
Peak Sample & Hold
Anti-Pile up Lockout
On-Chip Voltage References
Draws less than 3 mA @ +7V

Digital, Rad-Hard, CMOS Microcontroller

Flyback Power Supply ASIC

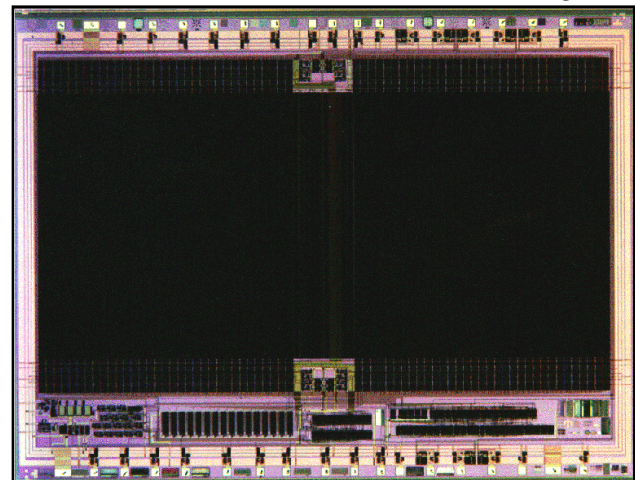


Mixed Signal, Rad-Hard, CMOS IC for Optical Imaging



32 channel, low-noise, differential amplifiers & threshold circuits
16-bit digital signal processor / 100 KHz, 10-bit A-to-D converter

Rad-Hard Non-Volatile Memory

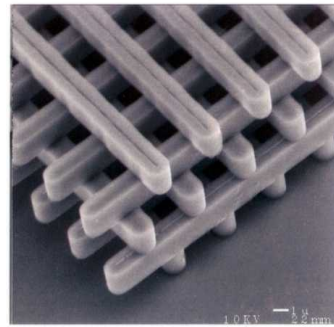


Transferred to Northrop-Grumman

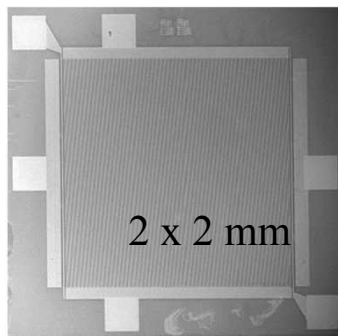


Sandia's Photonic Microsystems Technologies

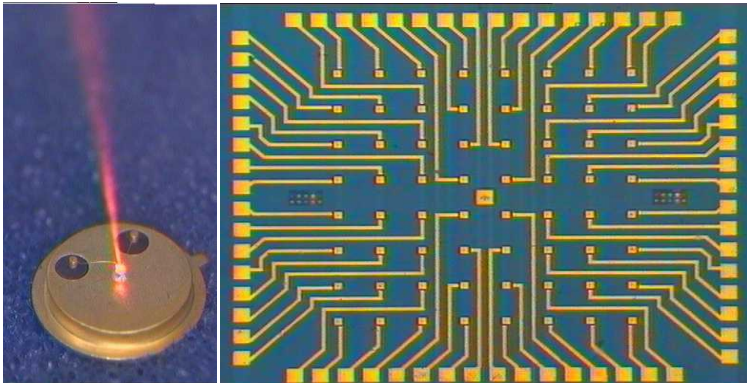
Photonic Crystals



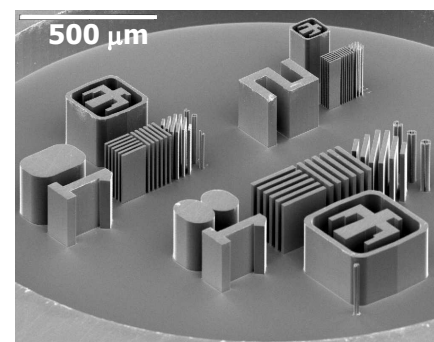
THz Detection & Quantum Cascade Lasers



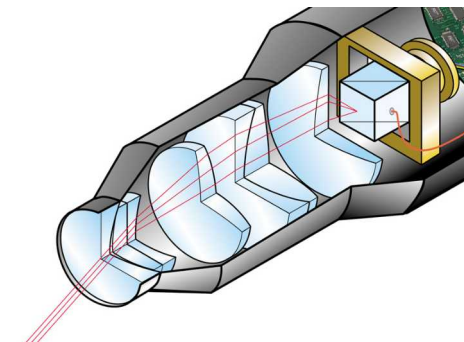
Visible & NIR VCSEL Arrays (Vertical-Cavity Surface-Emitting Lasers)



DXRL (LIGA)



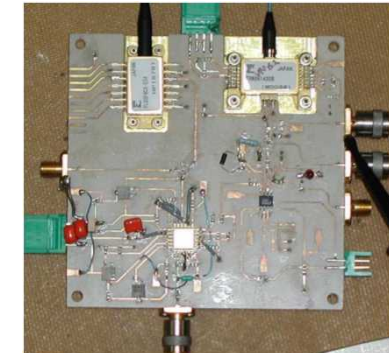
Optical Design



Subwavelength & Diffractive Optics



Novel Optical/Opto electronic Package and Test

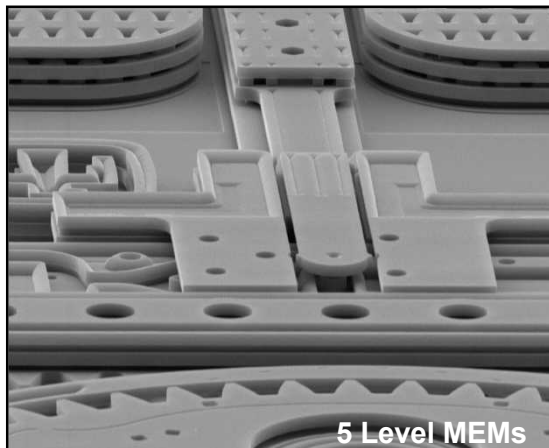


But, we are “technology agnostic” in our product developments

Micro-Mechanics Technologies

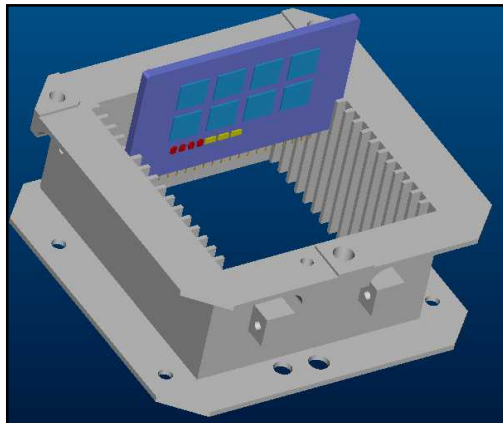
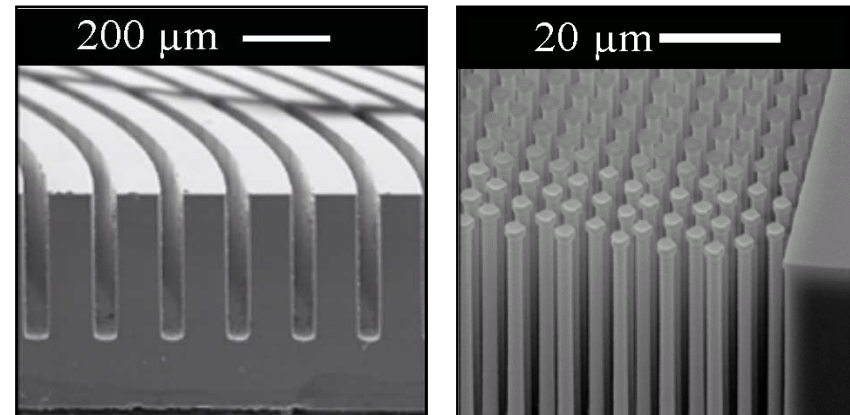
Silicon Surface Micro-Machining

1 micron x 8 micron



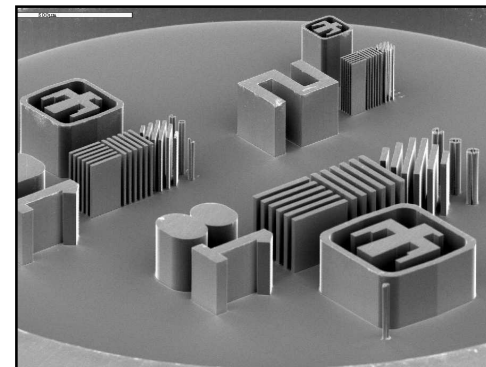
High Aspect Ratio Si Deep Reactive Ion Etching

5 micron x 200 micron

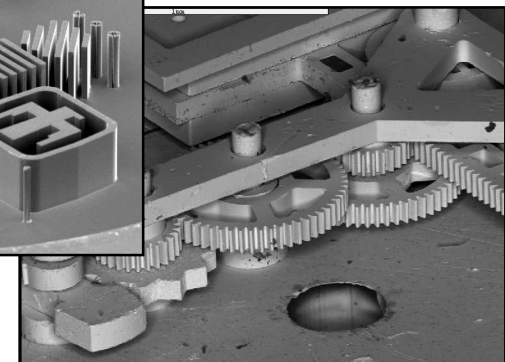


**Electro-
Discharge
Machining of
Metals**

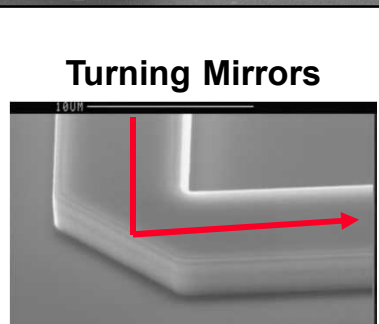
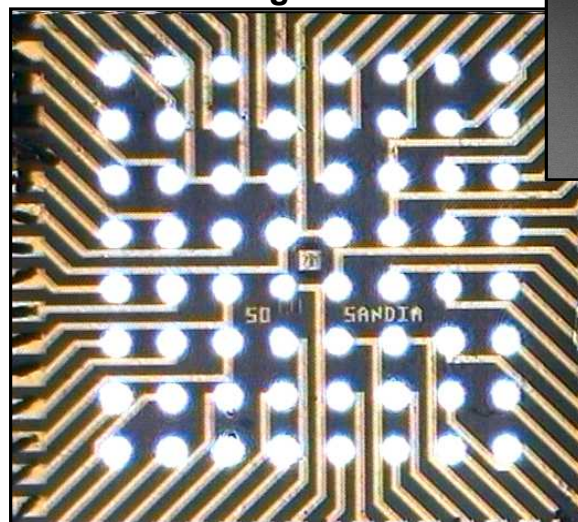
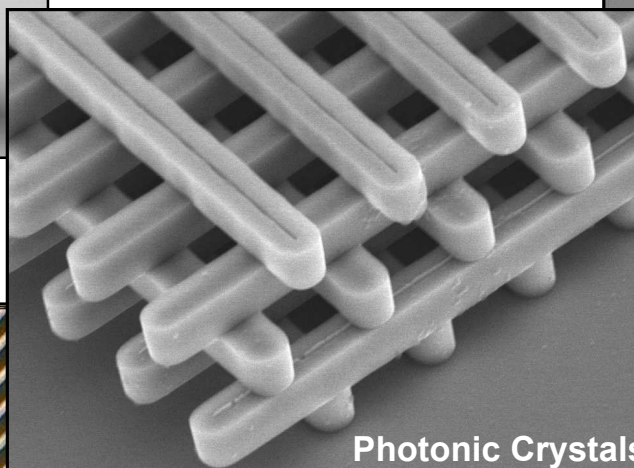
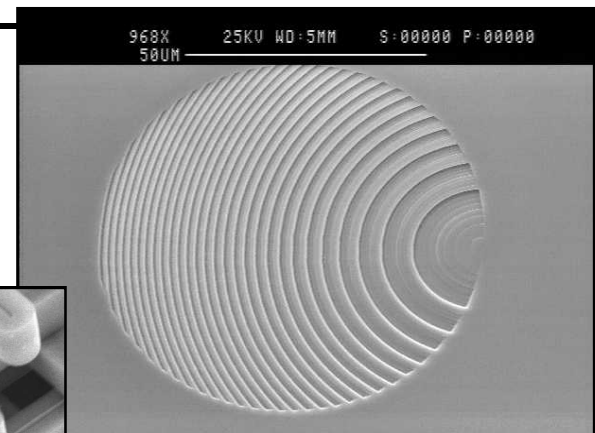
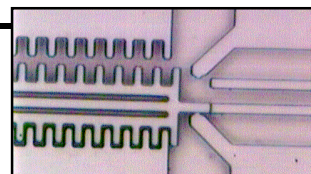
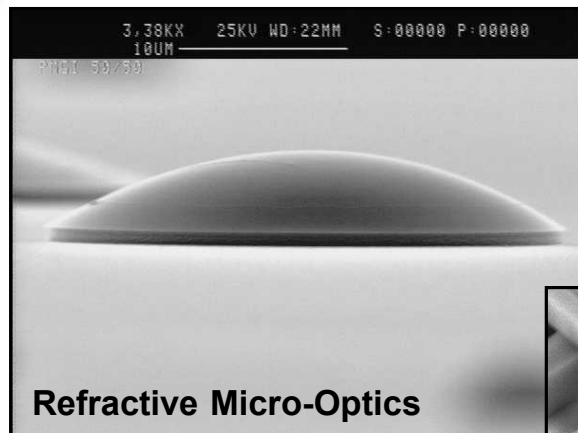
2 mil tolerances



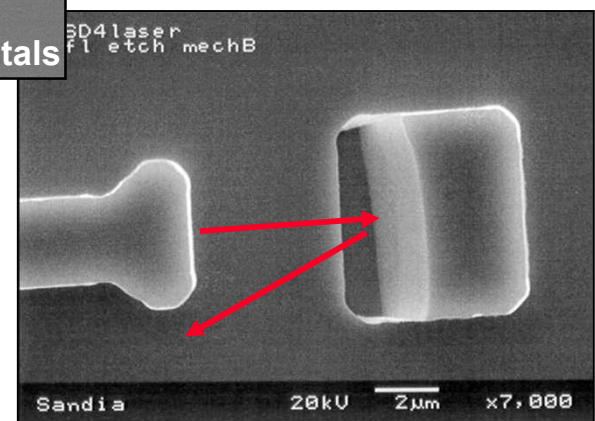
**LIGA Micro-
Machining, Metals**



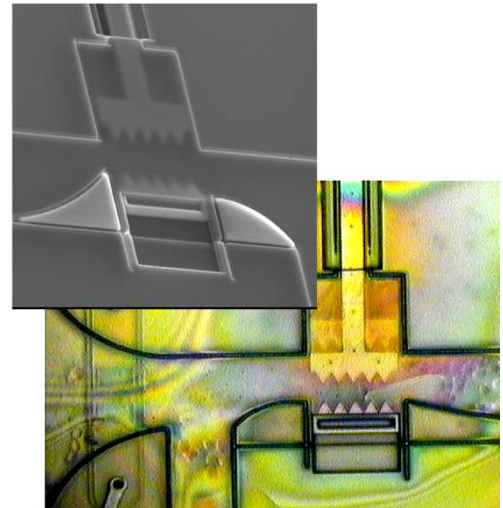
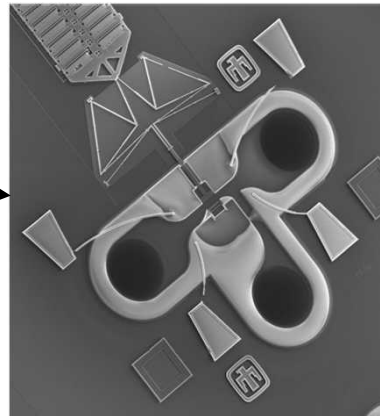
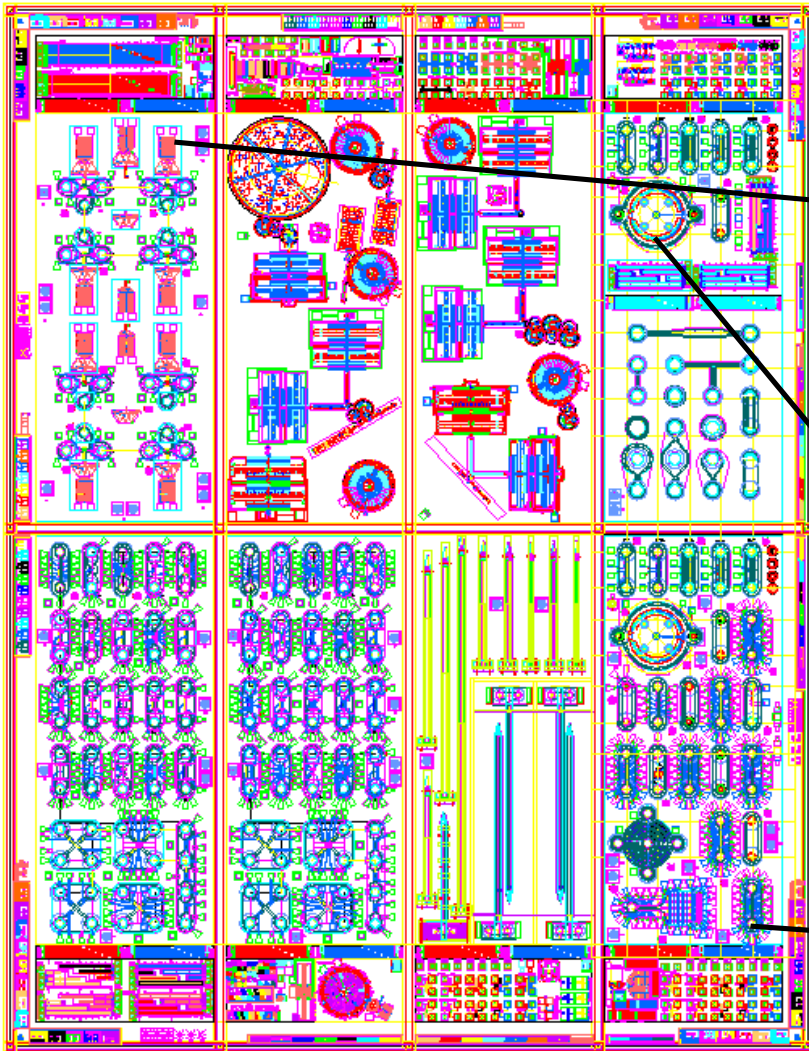
Micro-Optics Technologies



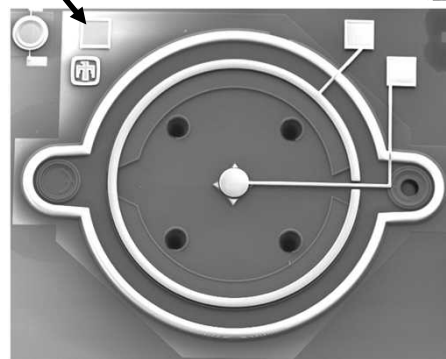
0.7 dB typ. excess loss



Surface Micromachined MicroFluidic Components

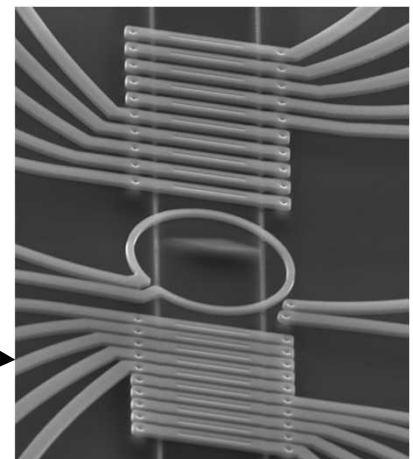


cellular manipulation



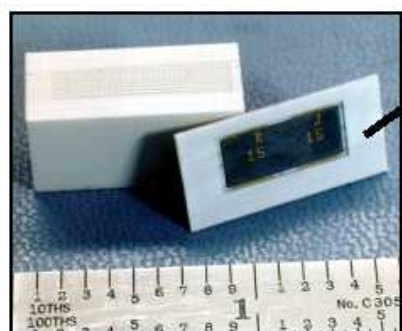
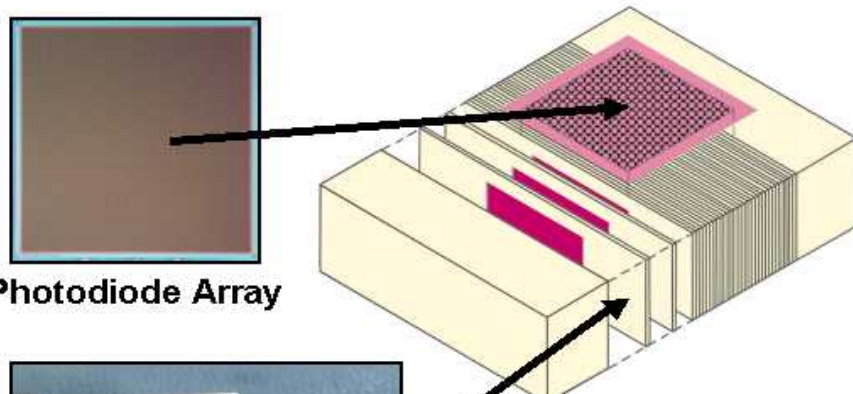
pumps

channels with
electrodes



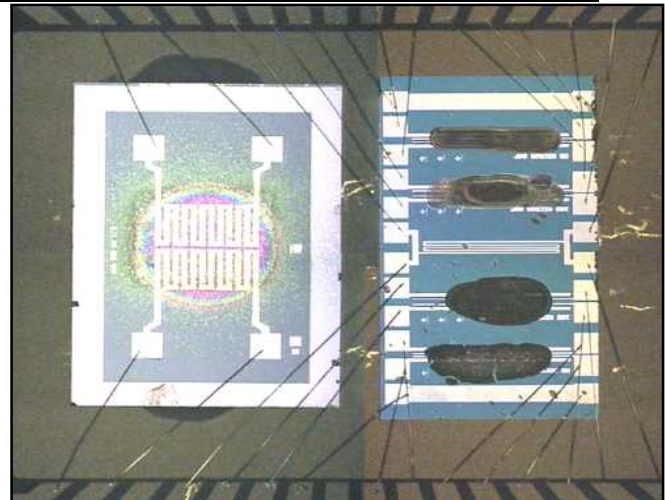
Micro-Packaging Technologies

3-D Assembly reduces size by a factor of > 1000

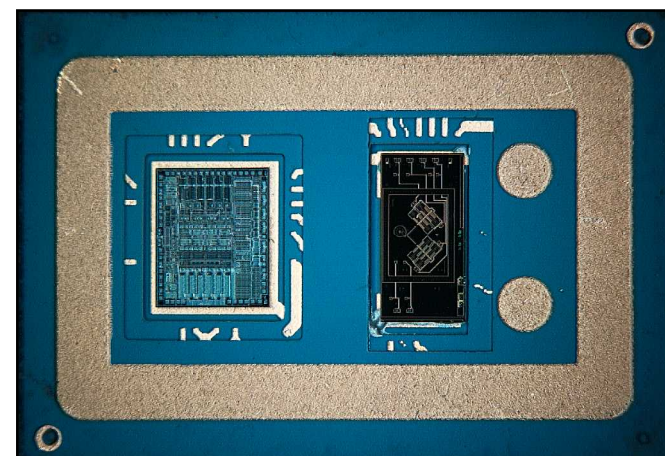


Mixed-Signal ASIC

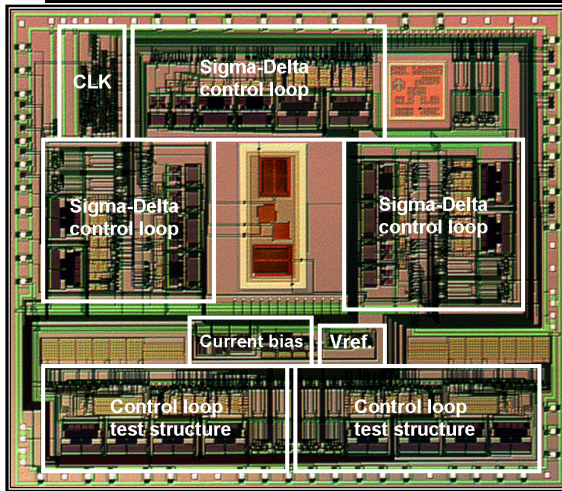
Low Temperature
Co-fired Ceramic
customized for
Hi-Rel microsystems



**Preconcentrator / ChemiResistor array
in Research Prototype package**

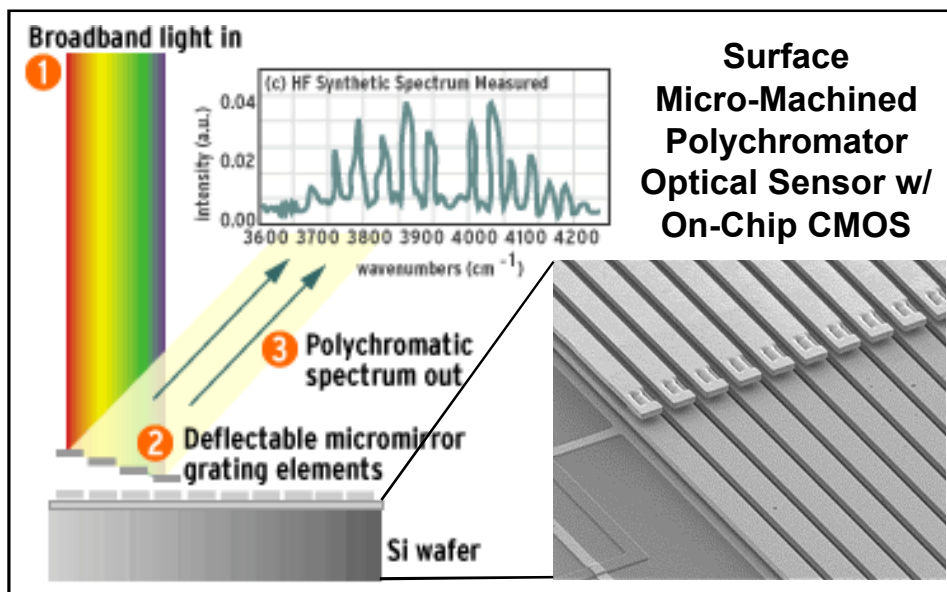
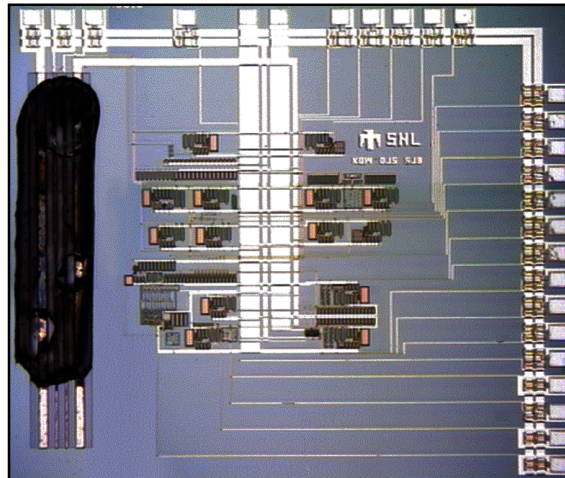


Integrated Sensor Technologies



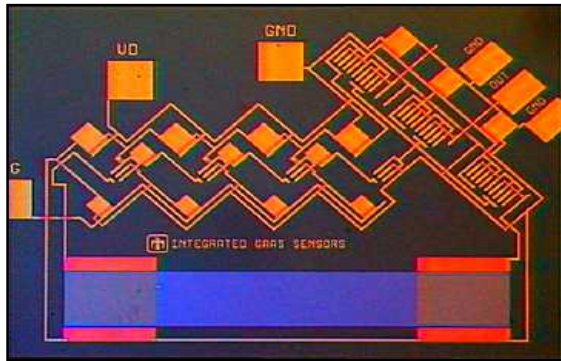
3-Axis Surface Micro-Machined Accelerometer w/ On-Chip CMOS

Chemi-Resistor Gas Sensor w/ On-Chip Mixed-Signal CMOS

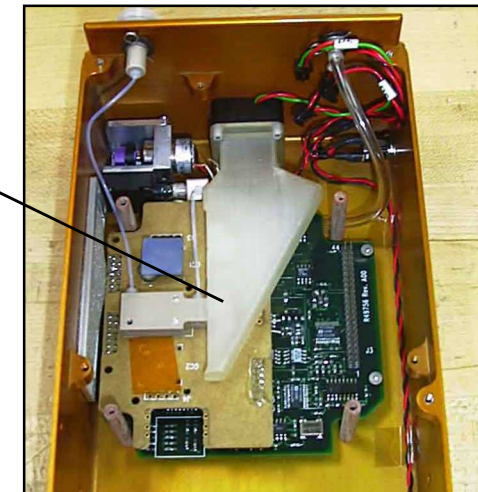
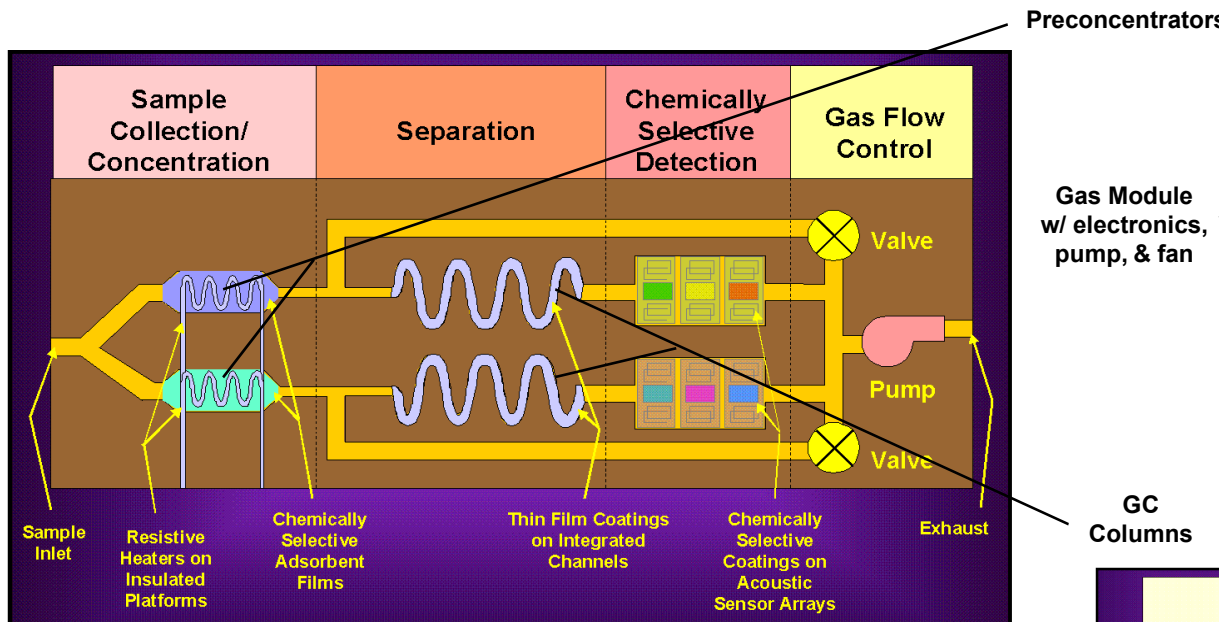


Surface Micro-Machined Polychromator Optical Sensor w/ On-Chip CMOS

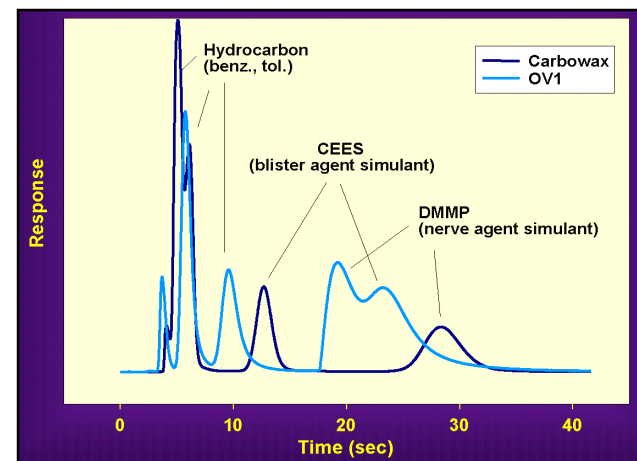
Surface Acoustic Wave Sensor w/ On-Chip GaAs Electronics



MicroChemLab Gas Analysis Module



GC
Columns



Gas Analysis Module Concept of Operation

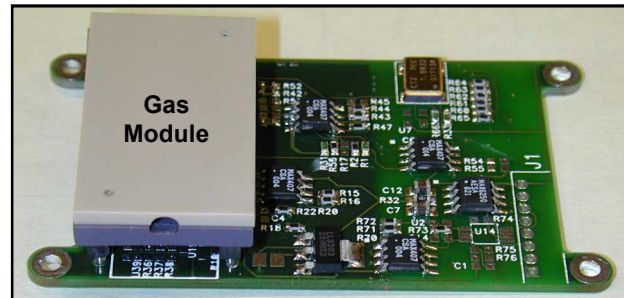
- 1) Selective preconcentrators are loaded by moving large volumes of air through them using bypass valves.
- 2) Valves are closed and a thermal pulse is applied to the preconcentrators to release the concentrated sample.
- 3) Time separation of gases occurs in gas chromatograph column.
- 4) Coated surface acoustic wave (SAW) detectors respond to gases.
- 5) Pattern recognition algorithms operate on the SAW data and identify and quantify the gas concentrations.

Silver Fox Mini-UAV with SnifferSTAR Gas Analysis Unit

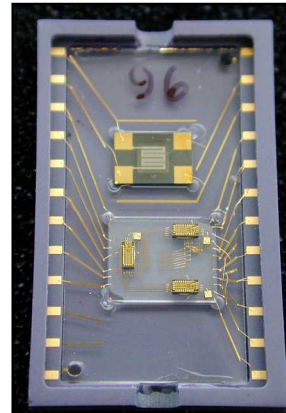


SnifferSTAR Gas Analysis Unit

- Detects blister agents and nerve agents
- Weight less than 16 grams
- Runs on 500 mW, peaking to 125 mA, +5V
- Total analysis time is less than 20 seconds
- Lockheed-Martin & Sandia National Laboratories



← 2.5" →



Gas Module
Without Lid



Award Winner for 2003

M. R. Daily, 1738
(505) 844-3145
dailymr@sandia.gov

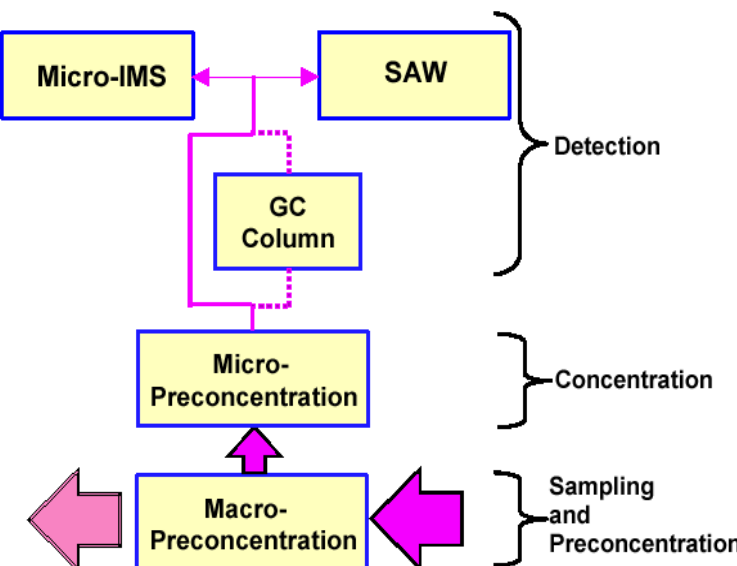
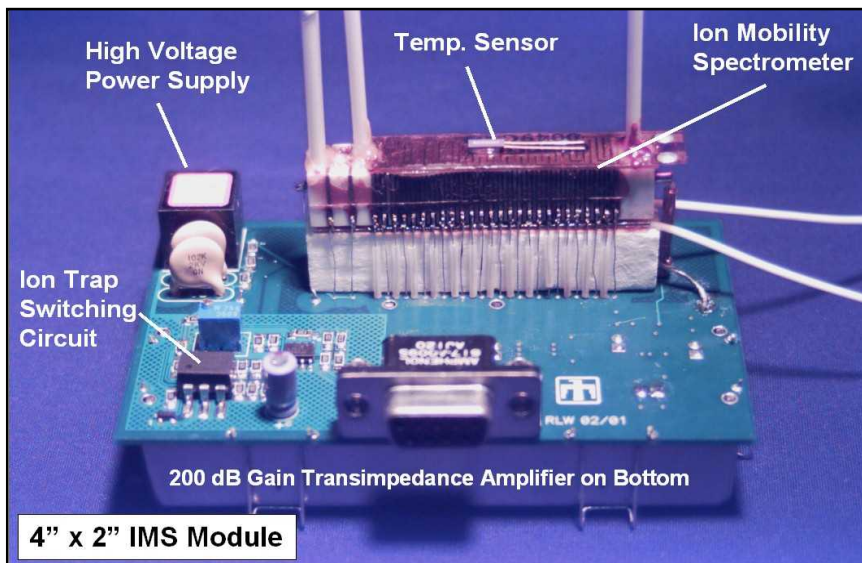
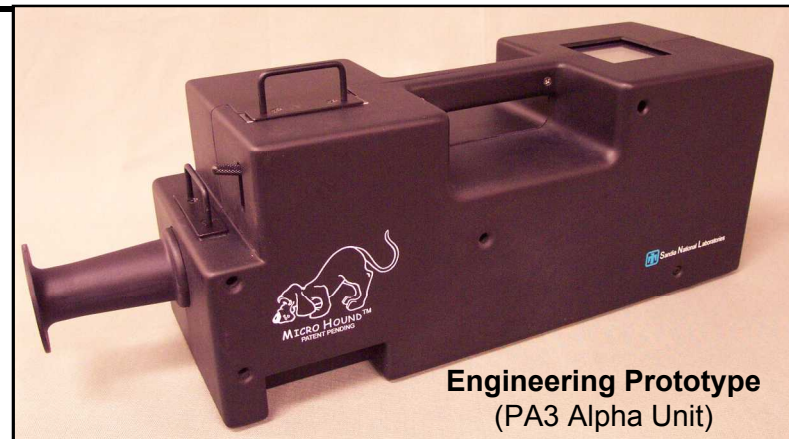


MicroHound

Explosives Detection System

MicroHound Explosives Detection Handheld Units

Ten MicroHound handheld explosive detection units have completed acceptance testing and have been delivered to the government customer. The MicroHound combines Center 4100's explosive sample collection and preconcentration technology with an Ion Mobility Spectrometer microsystem developed in Center 1700. The MicroHound is 1/4 the cost, 1/3 the weight (12 lbs), 1/2 the size, and has 4 times more single-charge operating life compared to competing products in the same performance class. It can detect trace amounts (nanograms) of explosives on equipment and people.





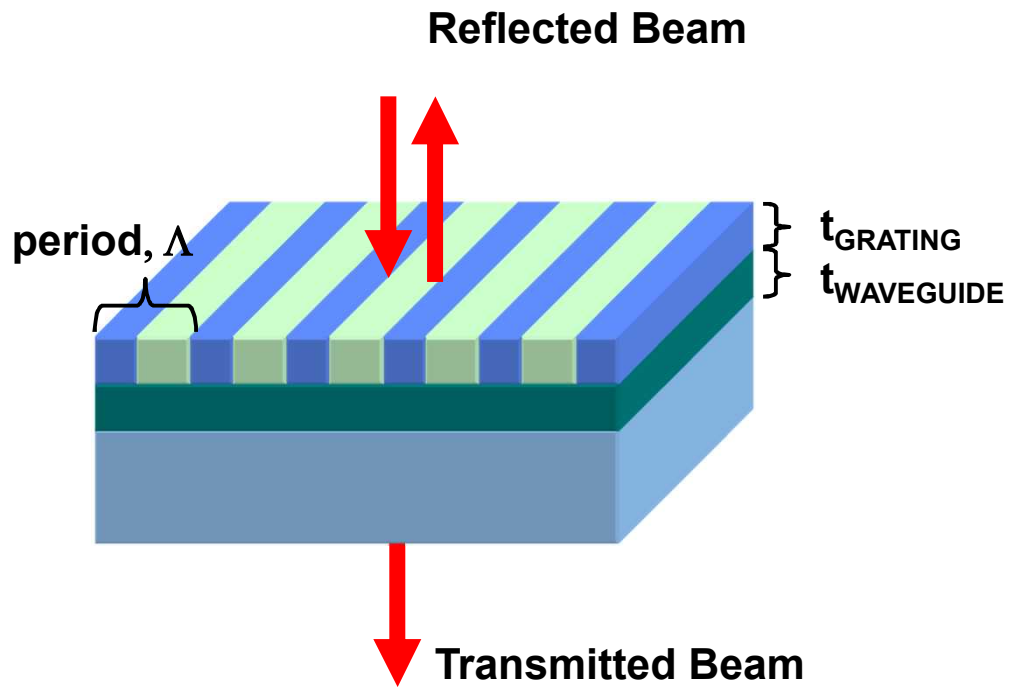
Low-sideband resonant subwavelength grating array design

D. W. Peters, S. A. Kemme, G.R. Hadley,
J. R. Wendt, T. R. Carter, and S. Samora

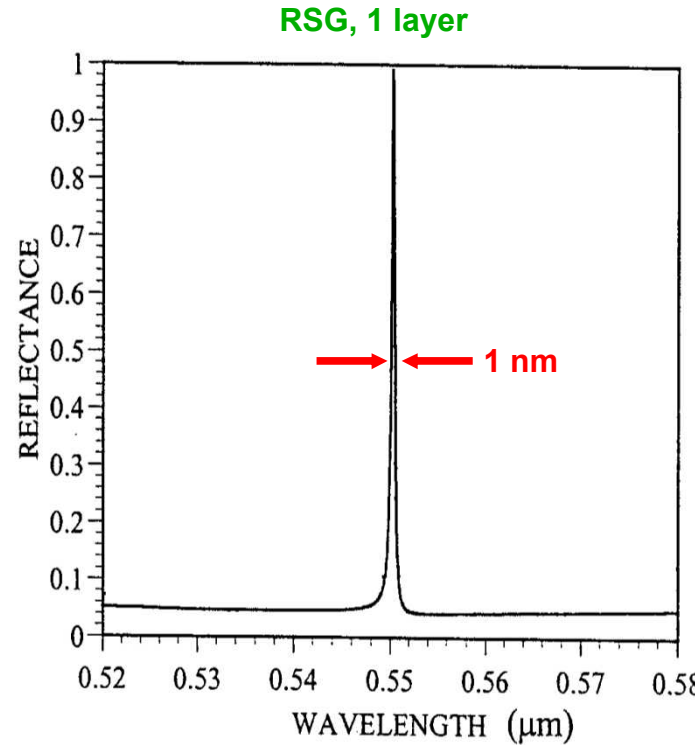
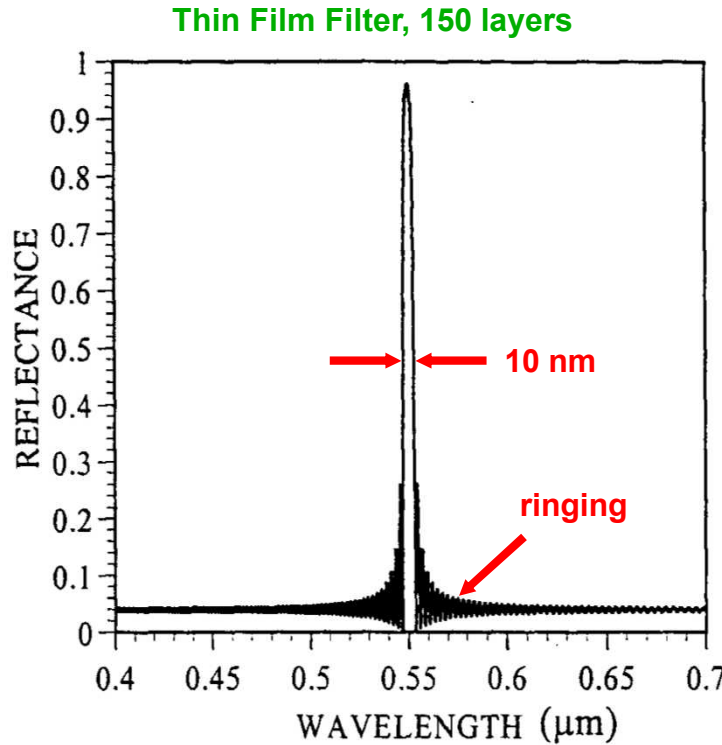
- Also called guided-mode resonant filters in the literature.
- Offers narrow wavelength band, narrow angular band reflector with low sidebands.
- Easier to pixelate than thin film filters.

Resonant Subwavelength Grating

- Light incident from above see a grating coupler and a waveguide.
- Light at specific angles, polarizations, and wavelengths can couple into the waveguide mode.
- The grating then couples this energy back out the top surface, leading to a reflected beam.



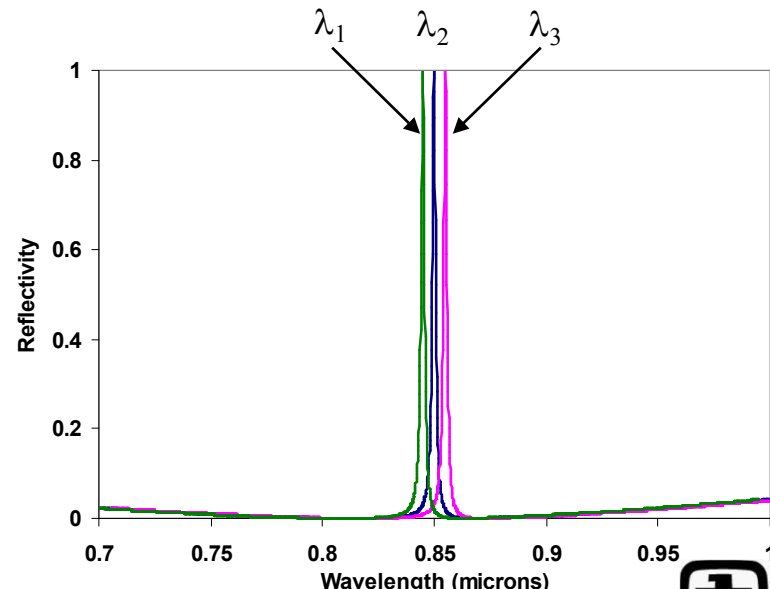
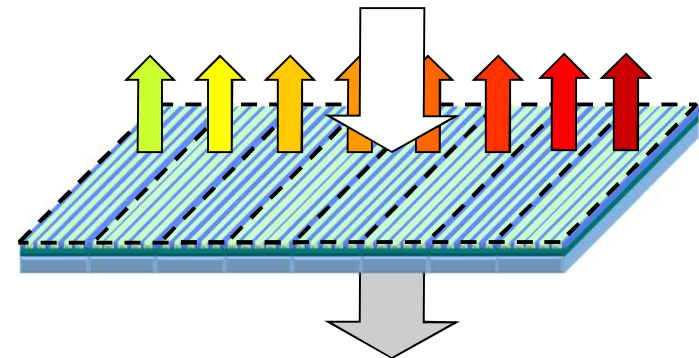
Comparison of Thin Film Filter to RSG



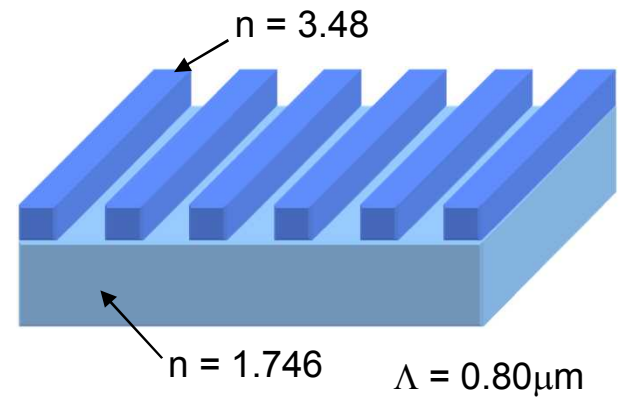
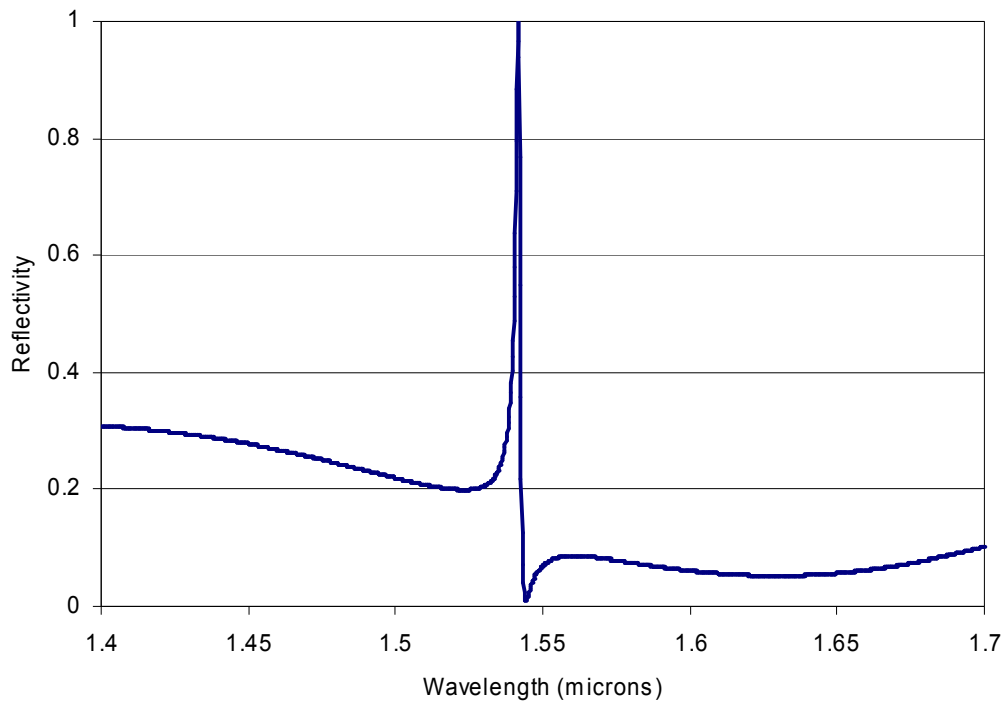
- Narrow wavelength band (0.01nm to 20nm) reflected 100%
- Reflected light in narrow angular band (~1mrad) for security applications
- Superior high efficiency and smooth sidebands, compared to thin film technology

Arrayed Subwavelength Resonant Gratings

- Easily implemented as pixilated, spectrally encoded array to match to detector array or chem/bio sensor array.
- FWHM of 1-2nm.
- Low sideband over wide range (0.7 to 1.0 μ m) for every pixel.



Typical Resonant Subwavelength Grating Reflectivity



Narrow resonant peak, but considerable sideband reflectivity
Unacceptable for an array



Variables in RSG Design

2-layer design allows AR-coat design for low sidebands.

Global variables

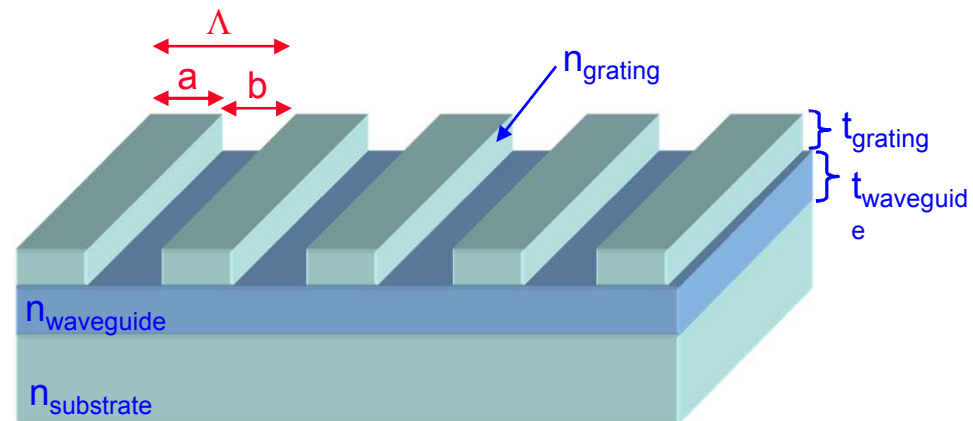
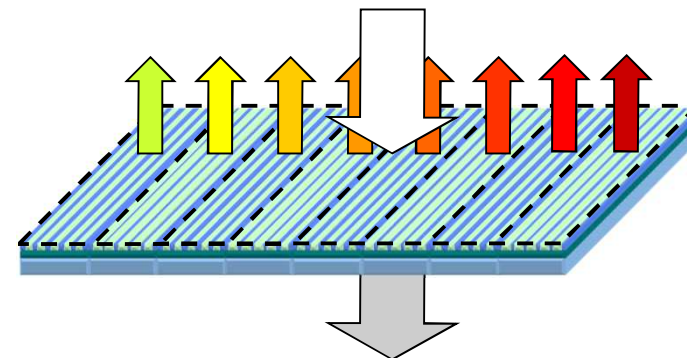
Indices of refraction

Layer thicknesses

Pixel variables

Grating period

Grating duty cycle
 $dc = a/(a+b)$





Material Choices

- **Fused silica substrate**

Robust material for visible and near-IR applications

- **TiO₂ waveguide layer**

Offers high index of refraction

Grown in-house or purchased from vendor

- **SiO₂ grating layer**

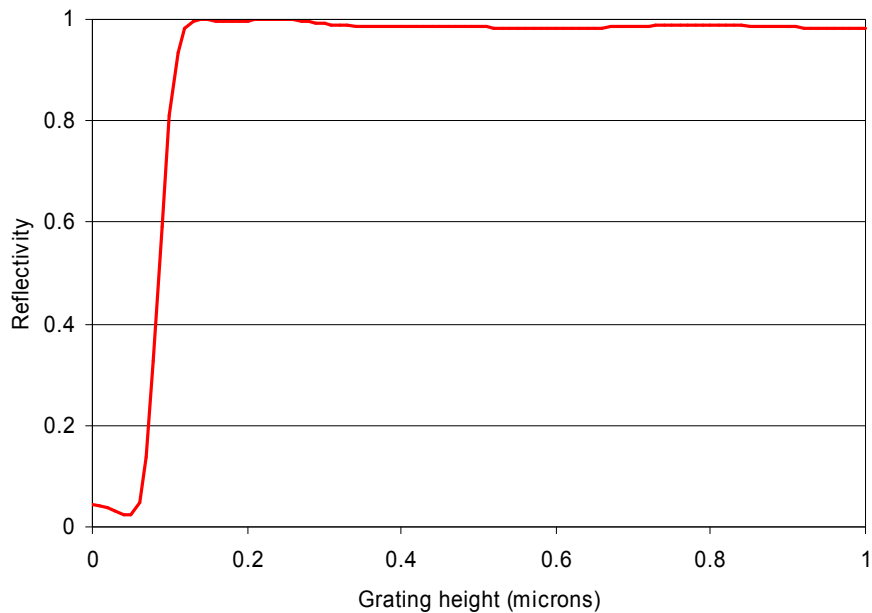
Relatively easy to deposit and etch

Mature in-house process

- **Chosen materials allow for effective AR coating**

Grating thickness determination

On-resonance reflectivity as a function of grating height



$$\lambda_0 = 850\text{nm}$$

$$t_{\text{waveguide}} = 185\text{nm}$$

$$dc = 0.4$$

$$n_{\text{grating}} = 1.4525$$

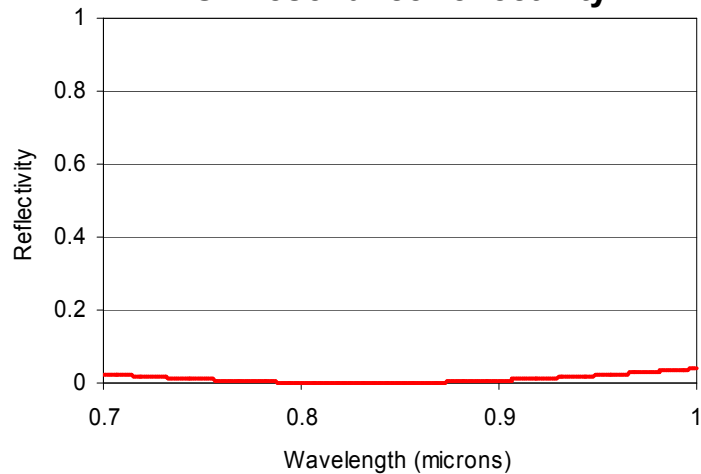
$$n_{\text{waveguide}} = 2.15$$

$$n_{\text{substrate}} = 1.4525$$

Resonance condition is relative insensitive to the grating height after $0.12\mu\text{m}$.

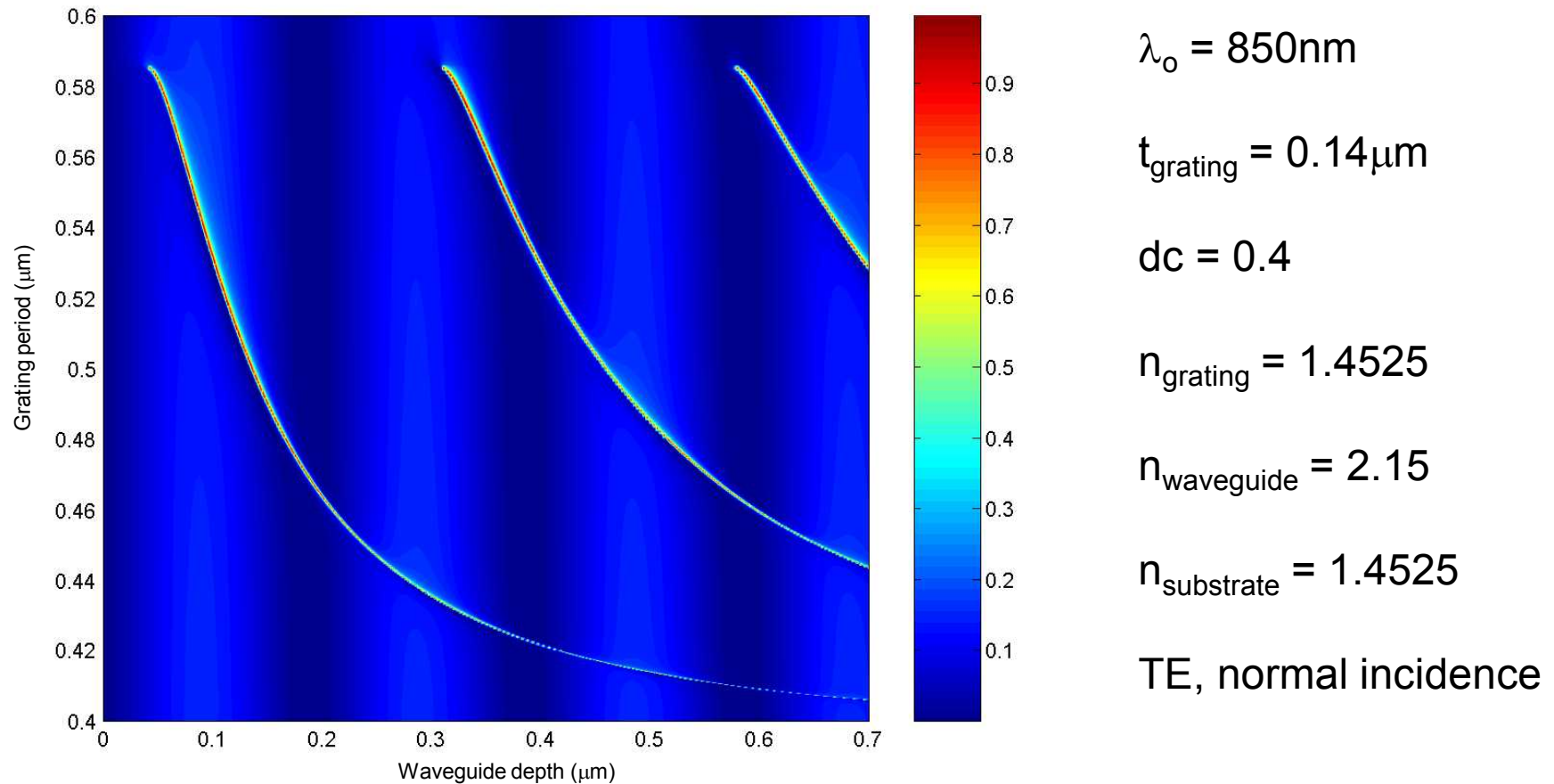
This allows us to use the grating height as a parameter in lowering sideband reflectivity.

Off-resonance reflectivity



- Replace the grating layer with a uniform layer with an equivalent effective index
- Optimize the thickness to minimize the reflectance near the center of the band

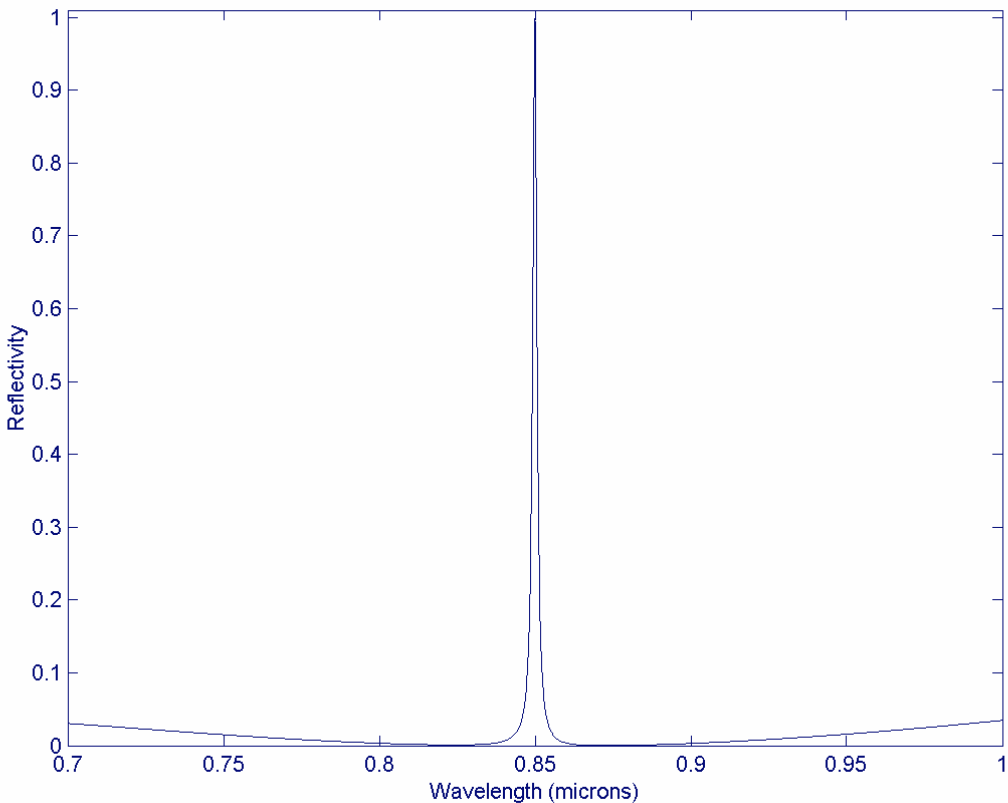
Reflectivity of infinite grating illustrating antireflection effect and resonant condition



Design around a point where the resonant condition coincides with a low background reflection



Reflectivity for an array pixel centered at 850nm

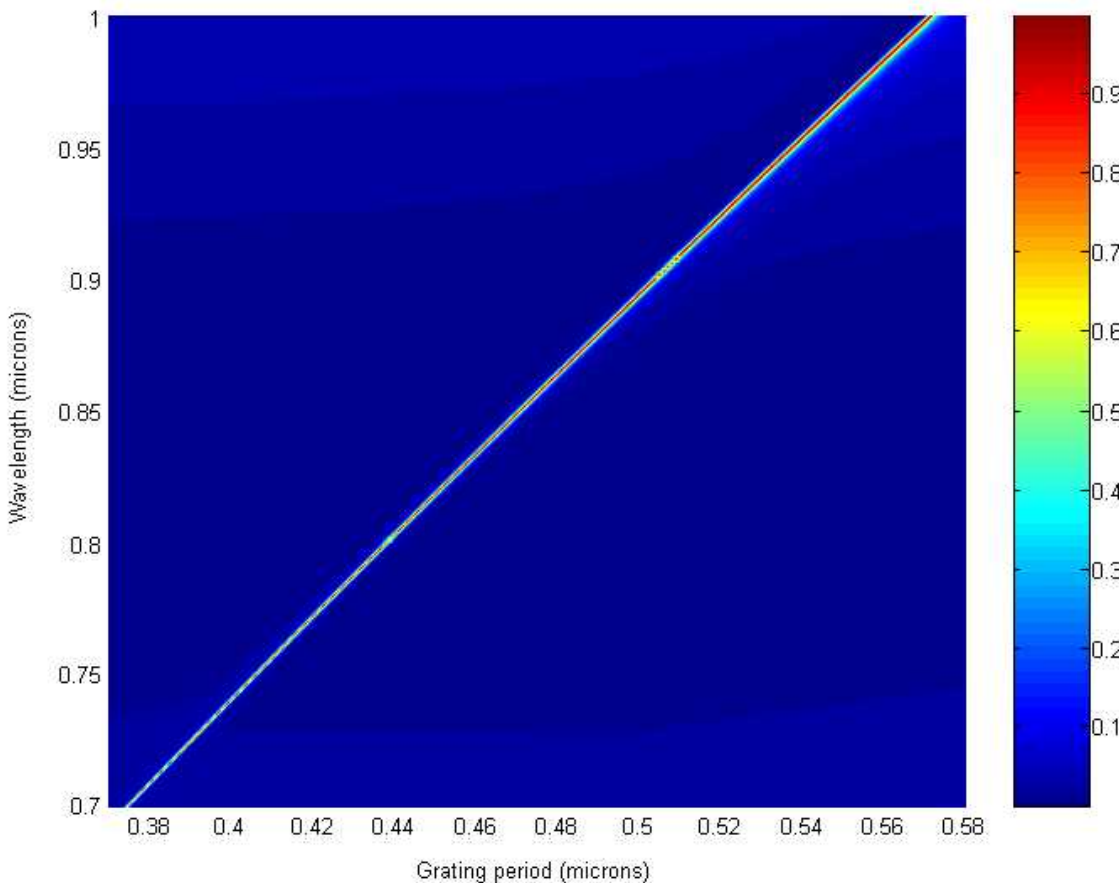


FWHM of 1.6nm.

**Reflectivity in sidebands
under 0.04.**

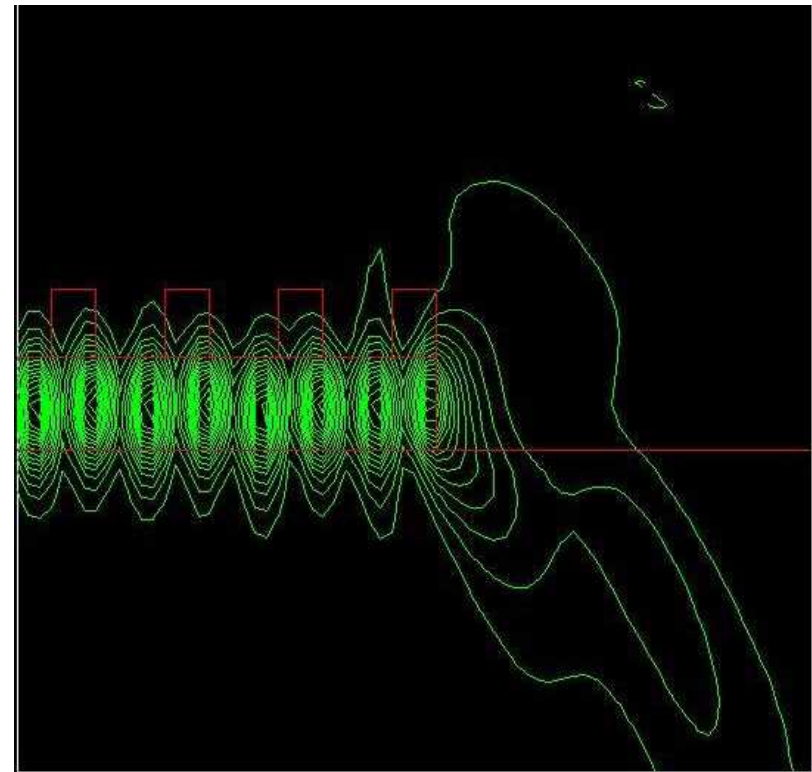
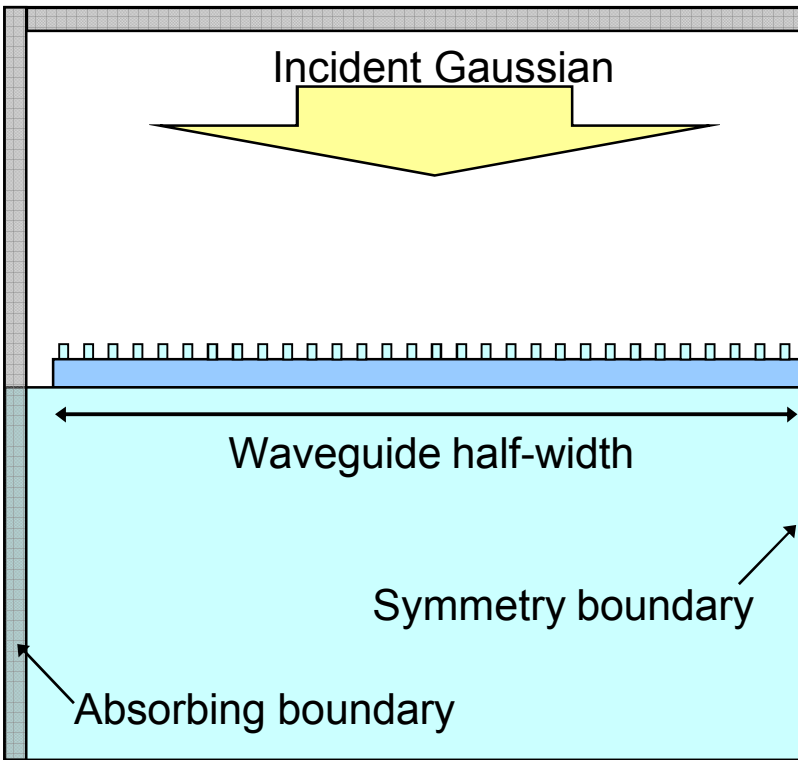
**Peak centered in
minimum of background
reflectivity.**

Tunability of resonant condition with grating period



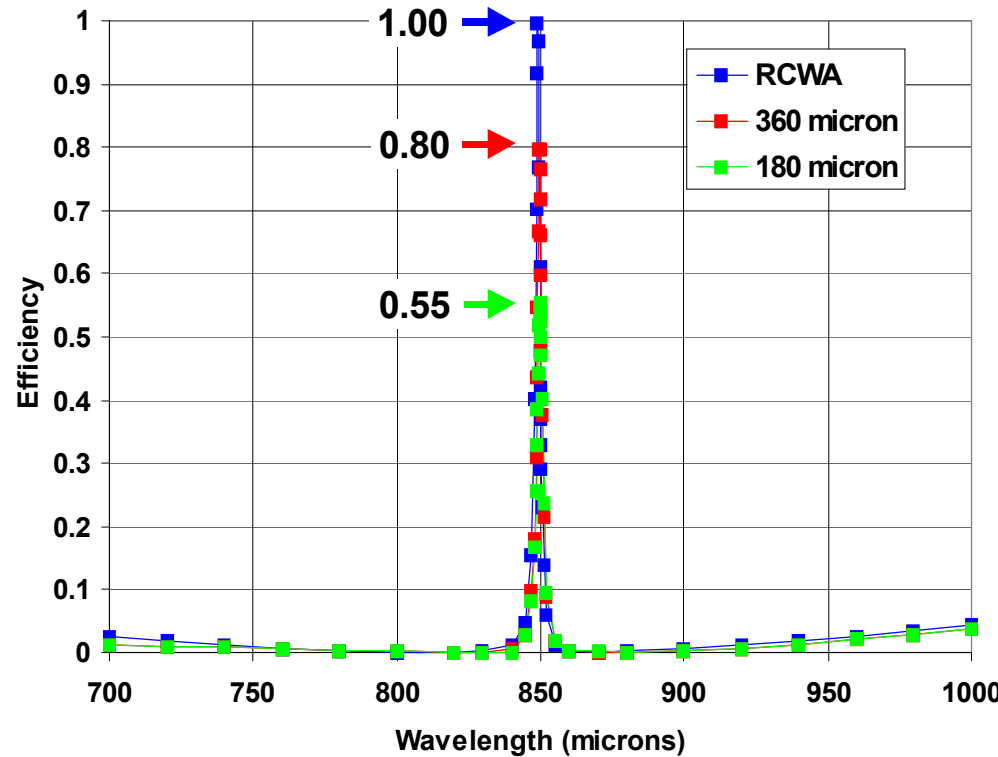
Linear variation of resonant wavelength with grating period while maintaining low sideband reflectivity

Modeling of finite extent gratings using Helmholtz finite difference method

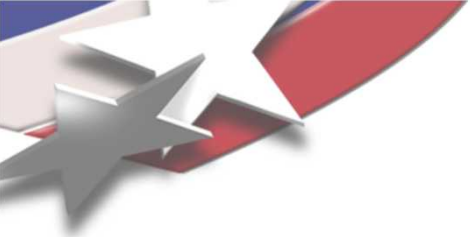


Reflection back into structure from end facet may enhance or degrade reflectivity depending on position of facet.

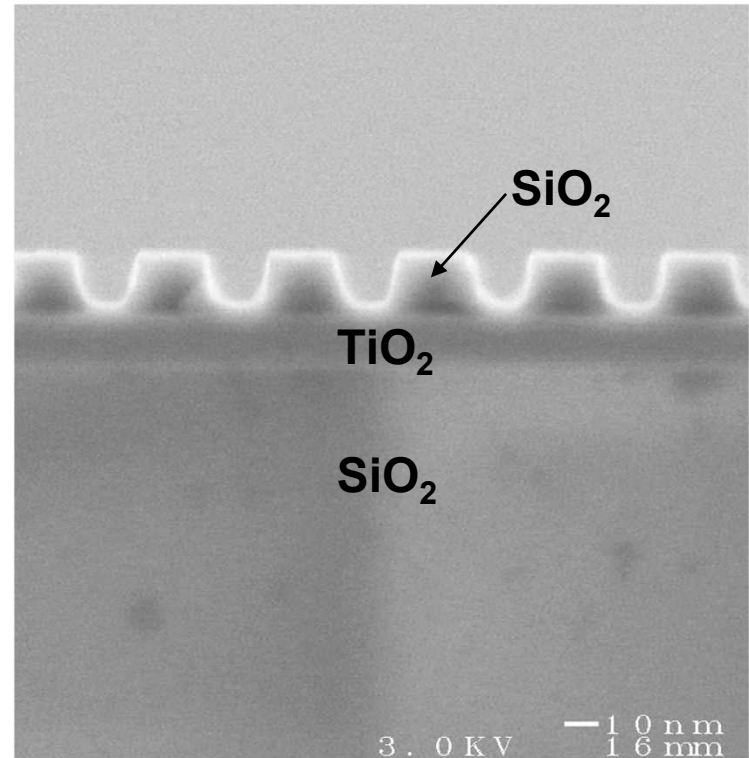
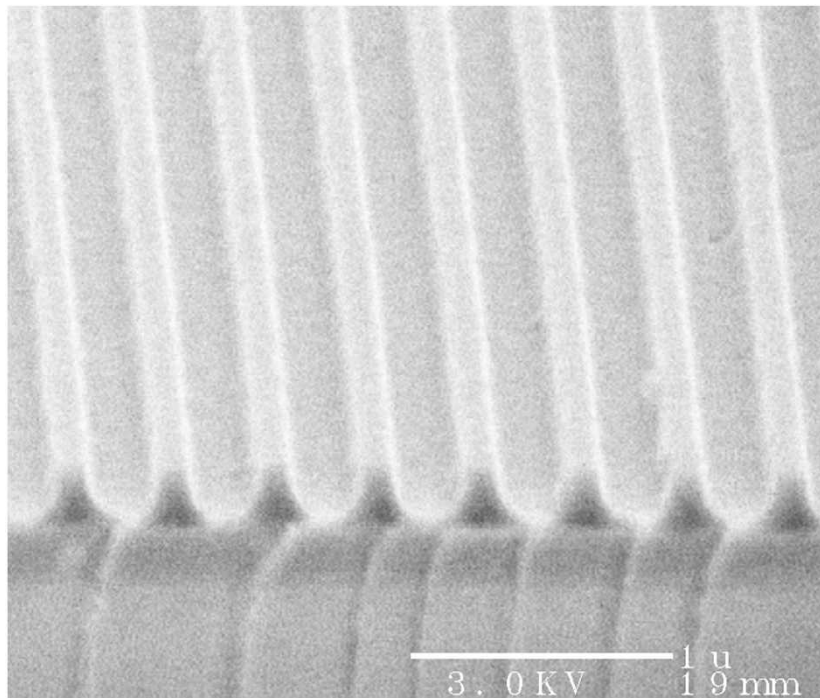
Effect of finite grating size



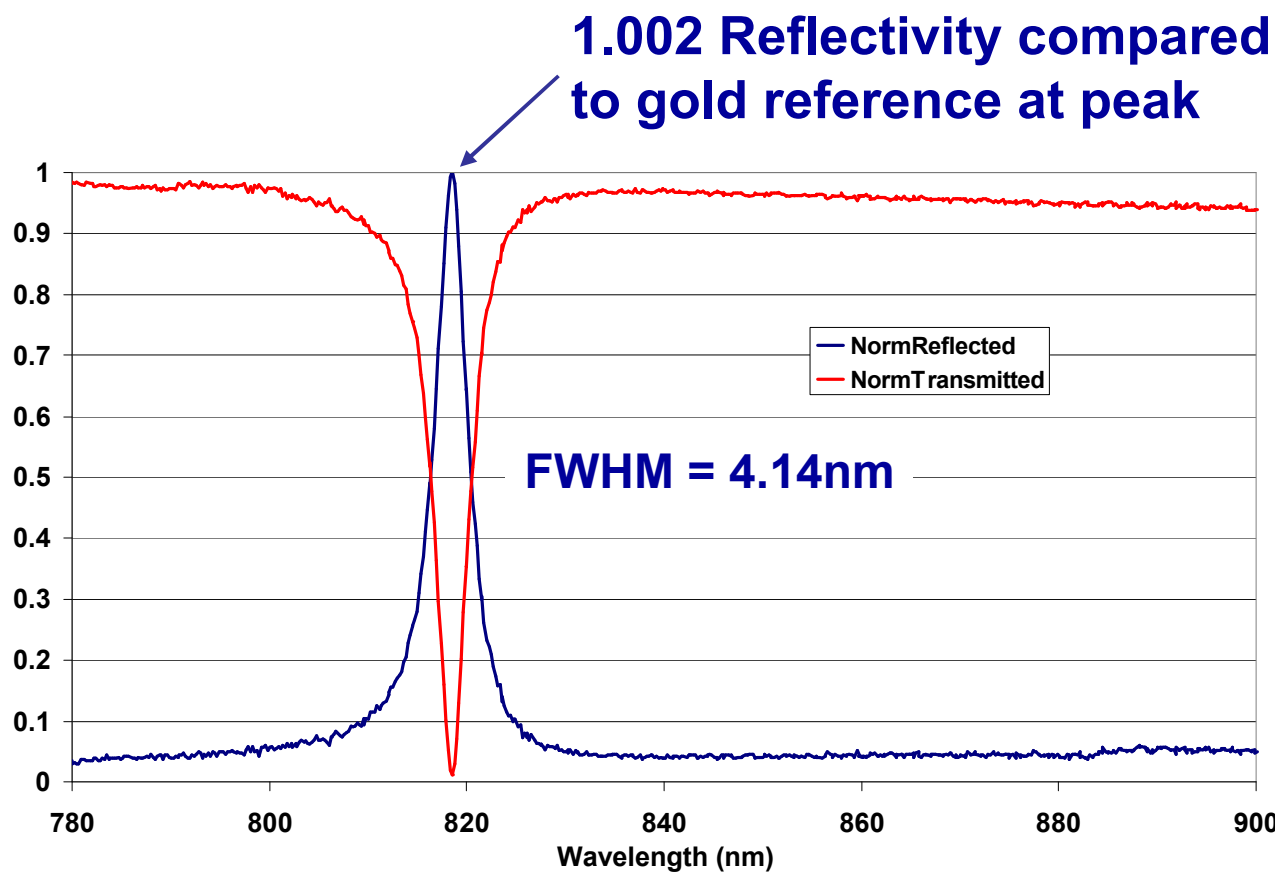
- Sideband reflectivity remains low
- FWHM only increases to 2.3nm for 180 μ m wide pixel



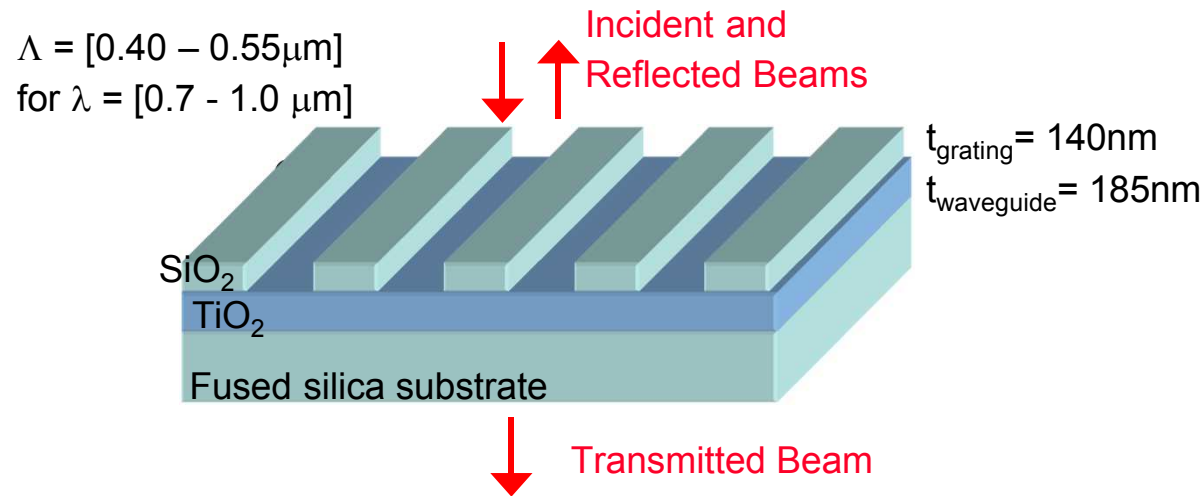
RSG SEMs



Measured Response



Summary



- Grating pitch linearly varies filter wavelength response
- Material and parameter configuration allows effective AR coat design for low sidebands across wide wavelength range
- Realistic modeling of finite-extent devices

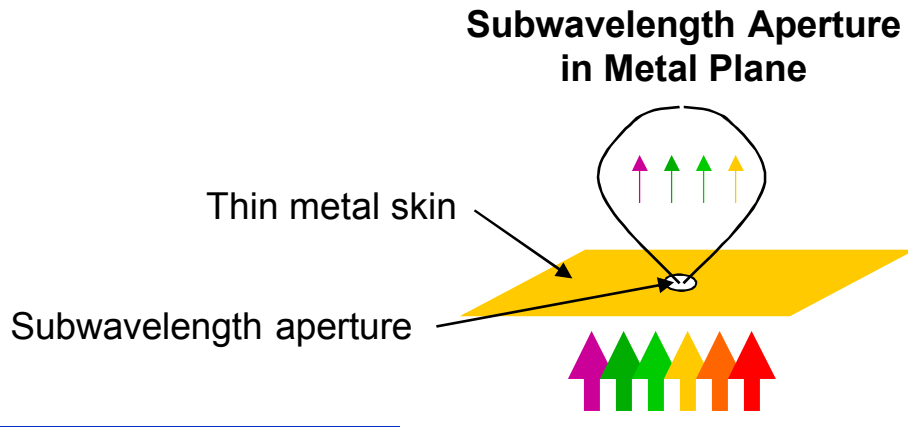


Surface Plasmon-Assisted Transmission and Emission from Subwavelength Patterned Apertures

David Peters, I. El-Kady, S. A. Kemme, and G. R. Hadley

Interesting surface wave effects in patterned apertures

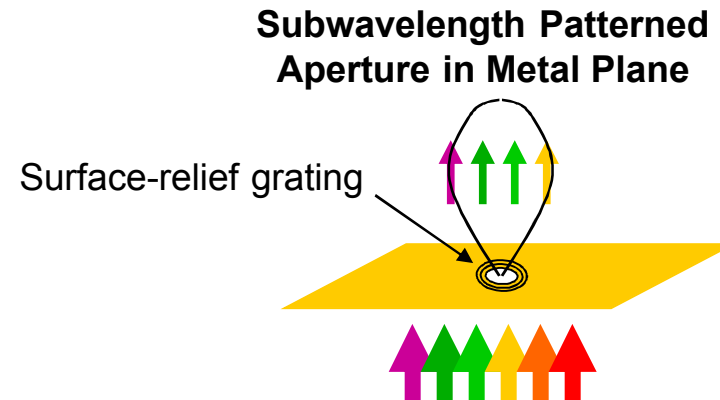
A small aperture in a metal surface allows very little light through.



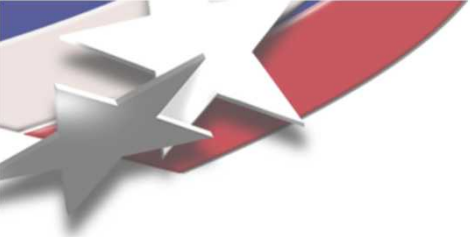
Patterning a surface-relief grating around the aperture allows much more light of certain wavelengths through the aperture.

Large enhancement factors reported.

Leads to an exit beam that beats the diffraction limit.



Applications in sensors, near-field microscopy, photolithography and data storage.

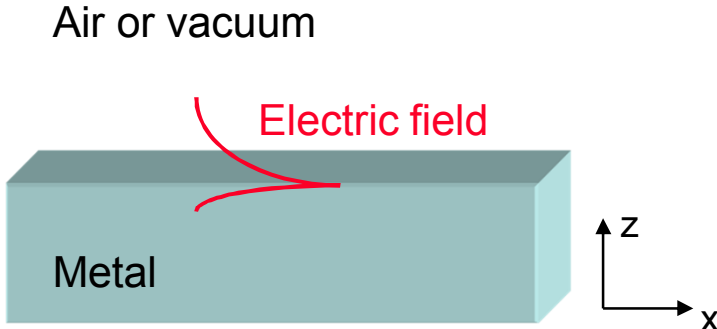


Surface Waves

Surface plasmons are electromagnetic fields that exist only at metal/dielectric interfaces.

It is impossible to directly couple to a surface plasmon with an incident photon at a uniform metal surface interface.

Highly dependent on surface properties.



$$E = E_o \exp[i(k_x x + k_z z - \omega t)]$$

k_x is real, therefore propagates.

k_z is imaginary, therefore decays exponentially.

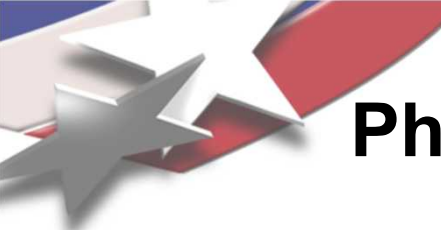
Examples of skin depth:

At air/gold interface at 1 μm :

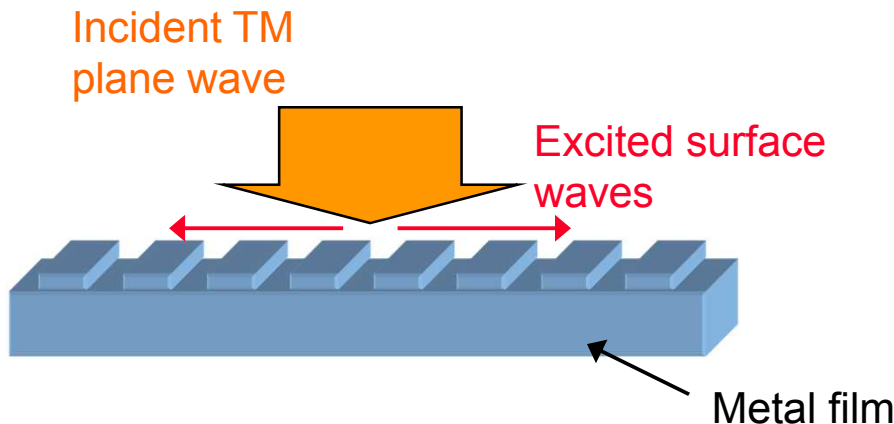
$$\delta_{\text{air}} = 1 \mu\text{m} \quad \delta_{\text{Au}} = 23 \text{ nm}$$

At air/silver interface at 500 nm:

$$\delta_{\text{air}} = 277 \text{ nm} \quad \delta_{\text{Au}} = 21 \text{ nm}$$



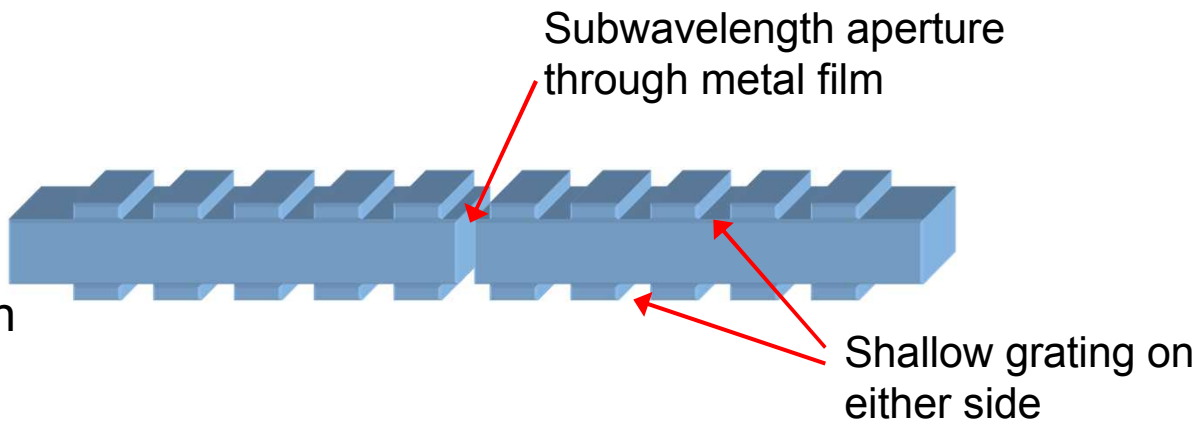
Photon-Surface Plasmon coupling



A metal grating matches the momentum of the incident wave to the evanescent surface waves, allowing coupling of energy.

Surface waves may travel along an aperture in a metal film.

A second grating may then couple to a propagating wave.





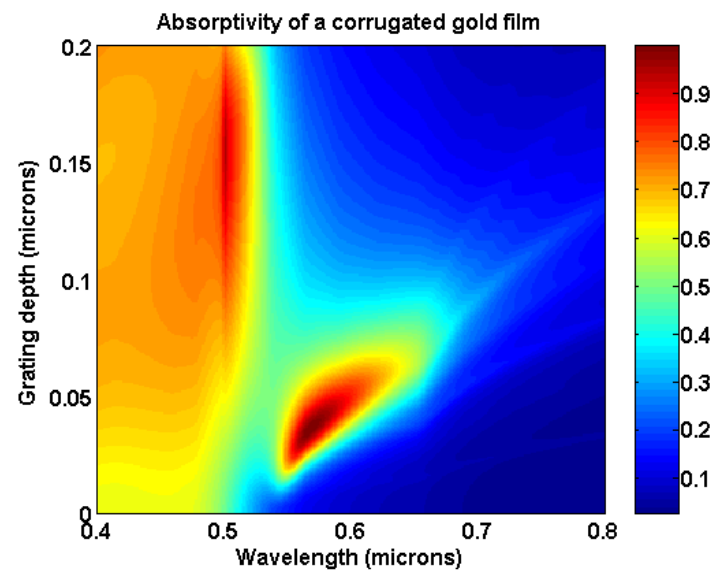
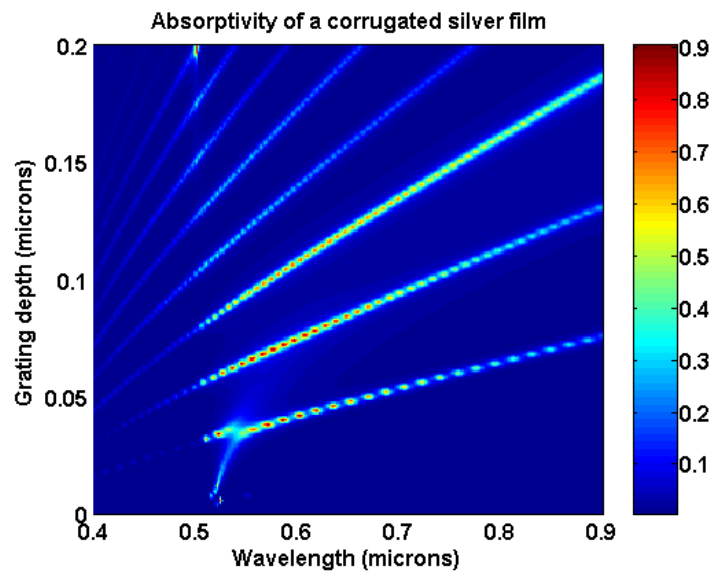
Modeling

Rigorous Coupled Wave Analysis (RCWA): Gives transmission, reflection, and absorption of infinite-extent gratings.

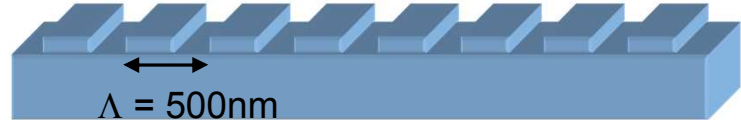
Finite Difference Implementation of the Semi-Vectorial Helmholtz equation: Shows near field patterns of finite-sized structures.

Transfer Matrix Method: Shows transmission and emission peaks.

Absorptivity of infinite-extent metal gratings modeled with RCWA

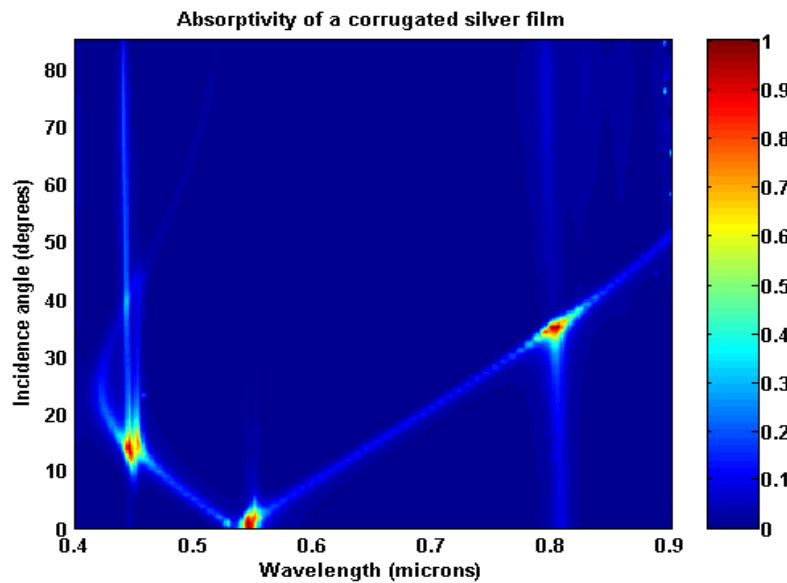


Illustrates the material issues involved in the visible portion of the spectrum.

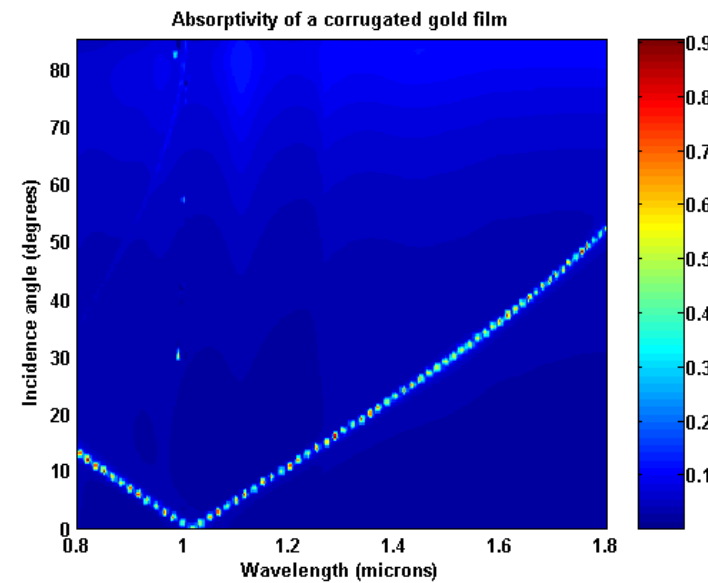


Absorptivity as a function of angle for infinite-extent grating

RCWA results for normal TM excitation



$$\Lambda = 500\text{nm}$$

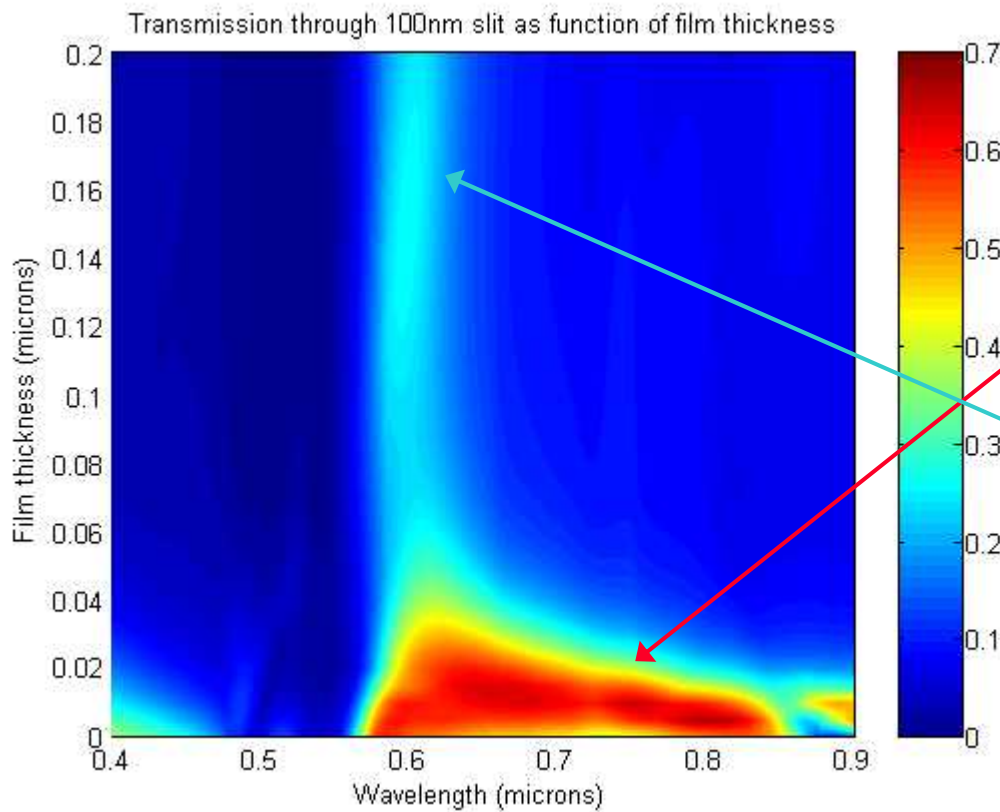


$$\Lambda = 1\mu\text{m}$$

RCWA modeling of single-sided gratings gives us a starting point for designing optimal structures.

RCWA results as function of film thickness

Metal film thickness

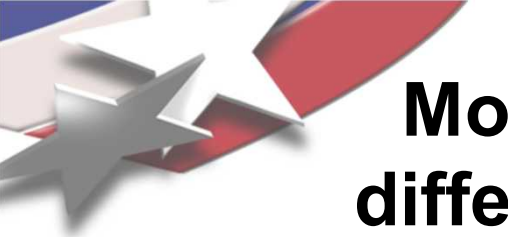


Front and back gratings have thickness of $0.06\mu\text{m}$.

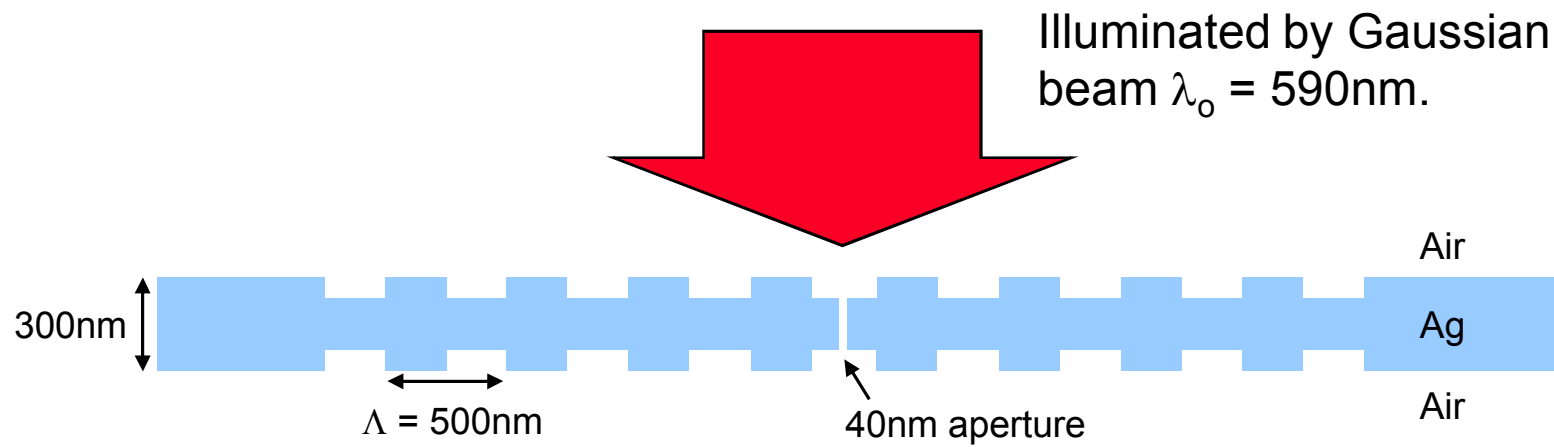
Aperture width: $0.1\mu\text{m}$

With an extremely thin film layer, light couples through the film over many wavelengths.

As the film thickness increases, only the wavelength coupled through the aperture by the surface waves is transmitted.



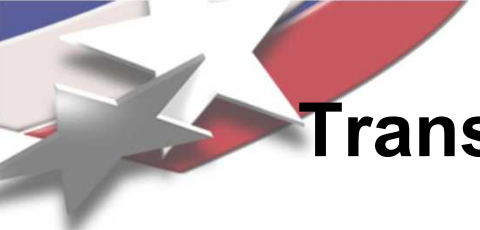
Modeling of near field with finite-difference Helmholtz equation code



Due to rapid extinction coefficient of the evanescent surface waves, a fine discretization of spatial coordinates is required for proper results. For these results $\Delta x = \Delta y = 5\text{nm}$.

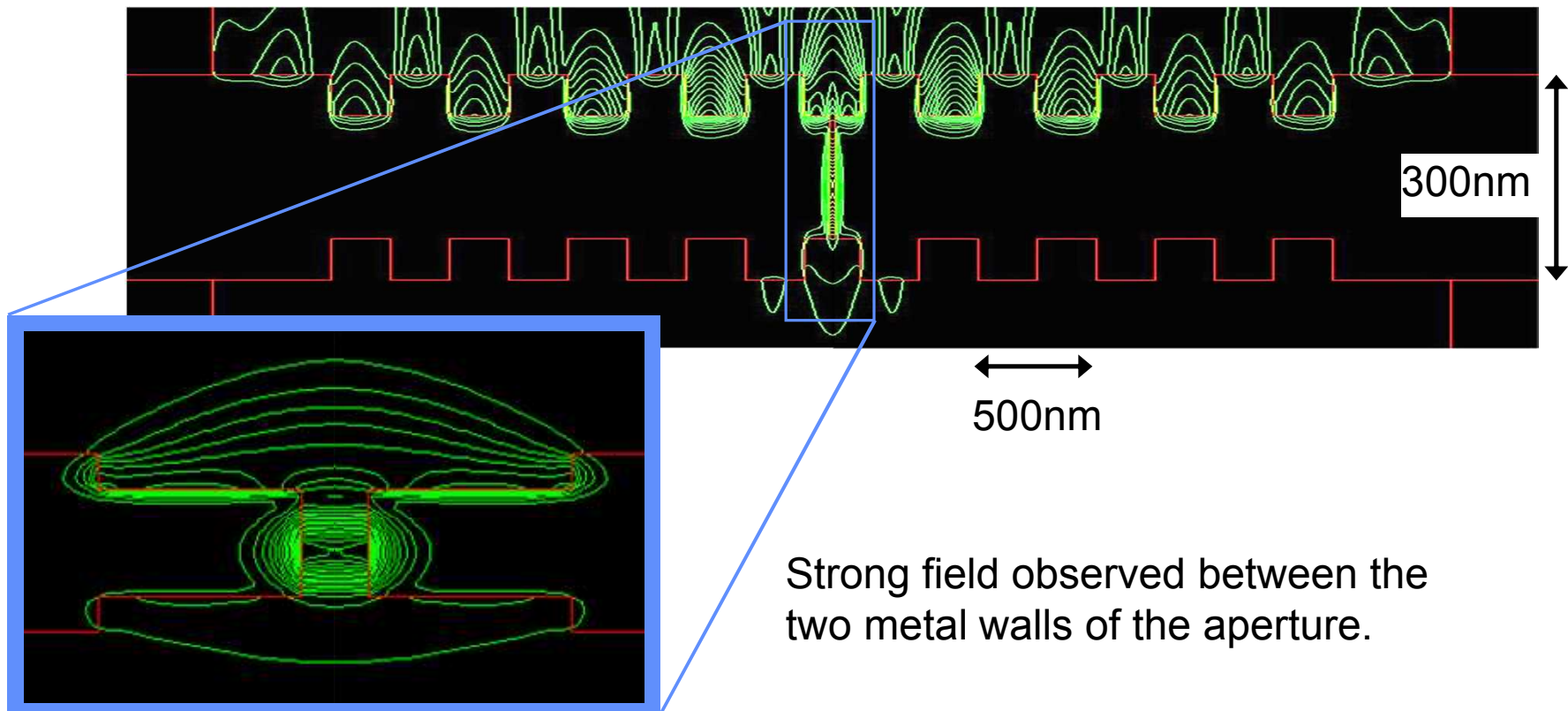
H. J. Lezec, A. Degiron, E. Devaux, R. A. Linke, L. Martin-Moreno, F. J. Garcia-Vidal, T. W. Ebbesen, "Beaming Light from a Subwavelength Aperture", *Science*, vol. 297, pp. 820-822, 2 Aug. 2002.

H. J. Lezec, T. Thio, "Diffracted evanescent wave model for enhanced transmission through subwavelength hole arrays," *Opt. Express*, vol. 12, p. 3629, (2004).

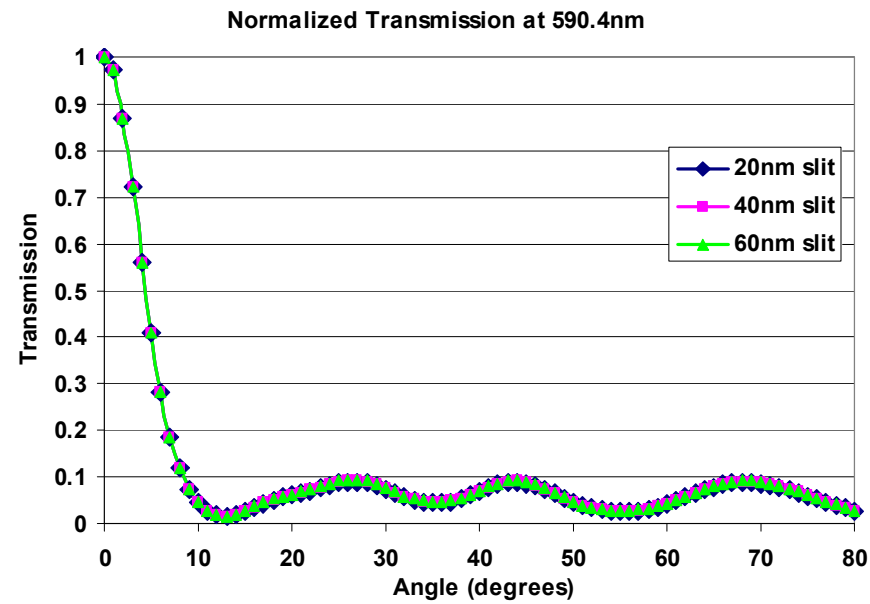
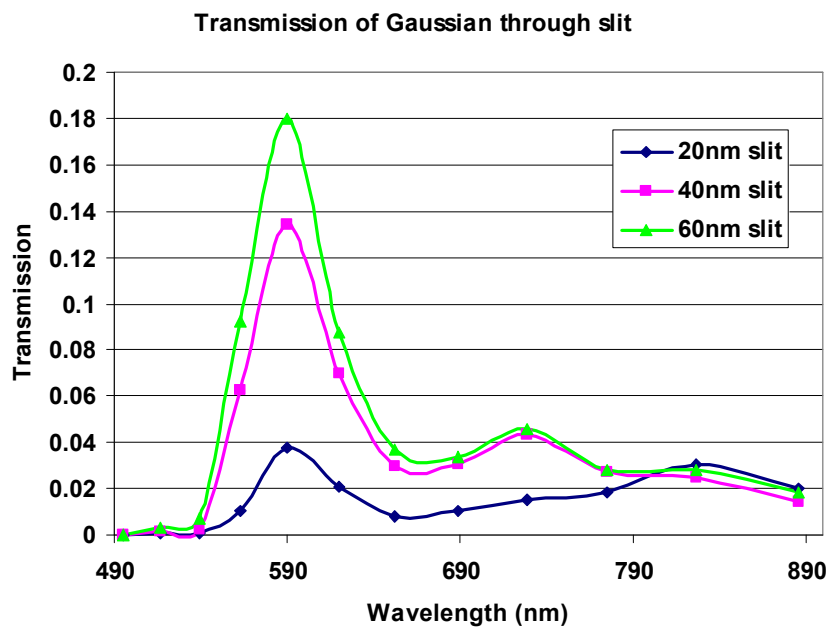


Transmission through 40nm aperture

FDM Helmholtz code results:

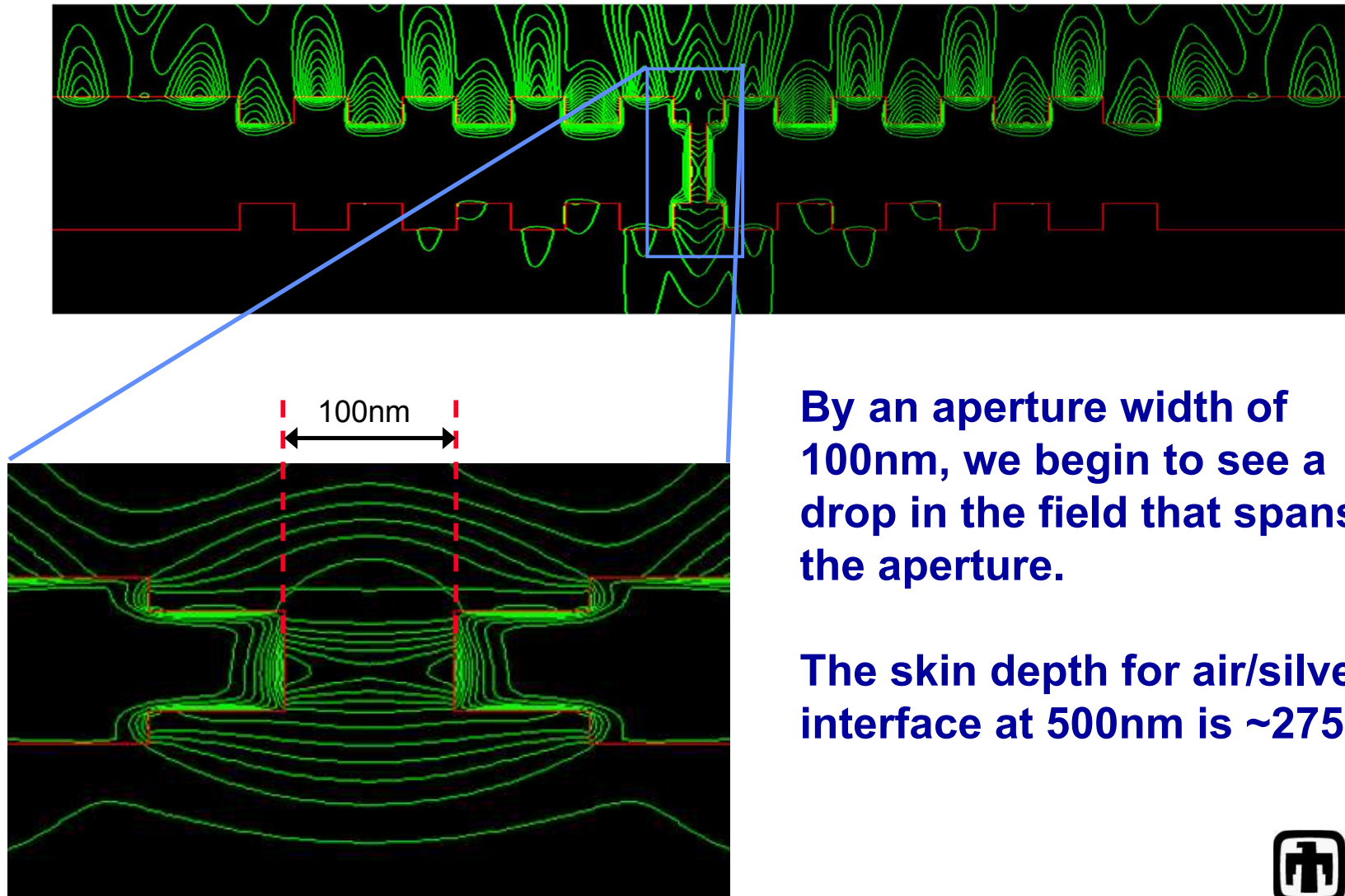


Comparison of transmission for three slit widths



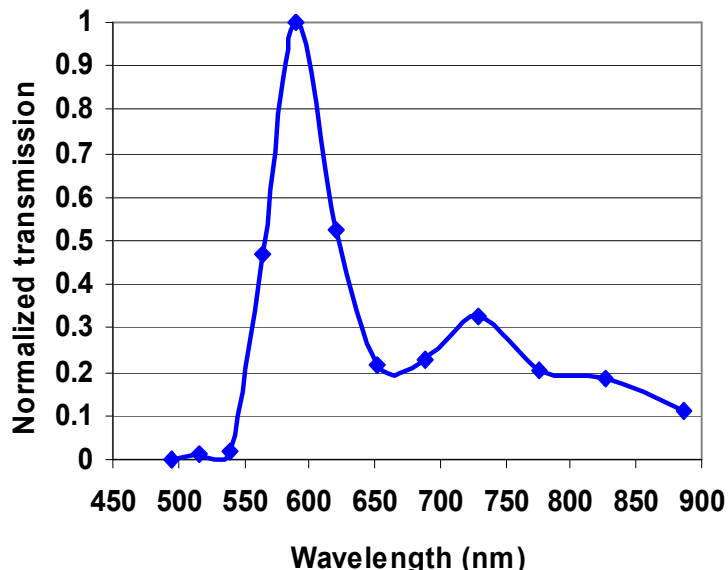
Although the spectral response varies with aperture width, the angular divergence at 590.4nm is near identical.

Increase of aperture width increases transmission to a point

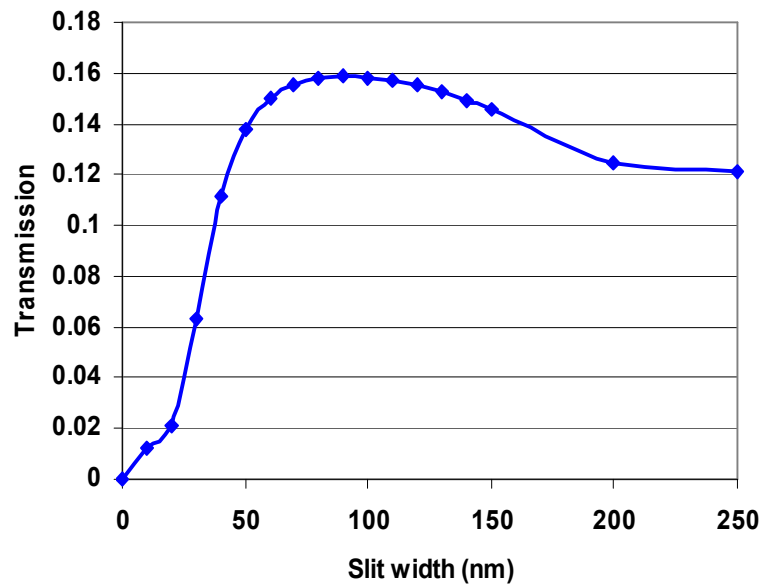


Optimization of aperture width

While the period can be adjusted to shift the transmission peak in the spectrum, the grating depths and aperture width can be optimized to maximize this transmission.



Normalized transmission of a $4\mu\text{m}$ -wide Gaussian through a 40nm linear aperture in silver film as a function of wavelength.

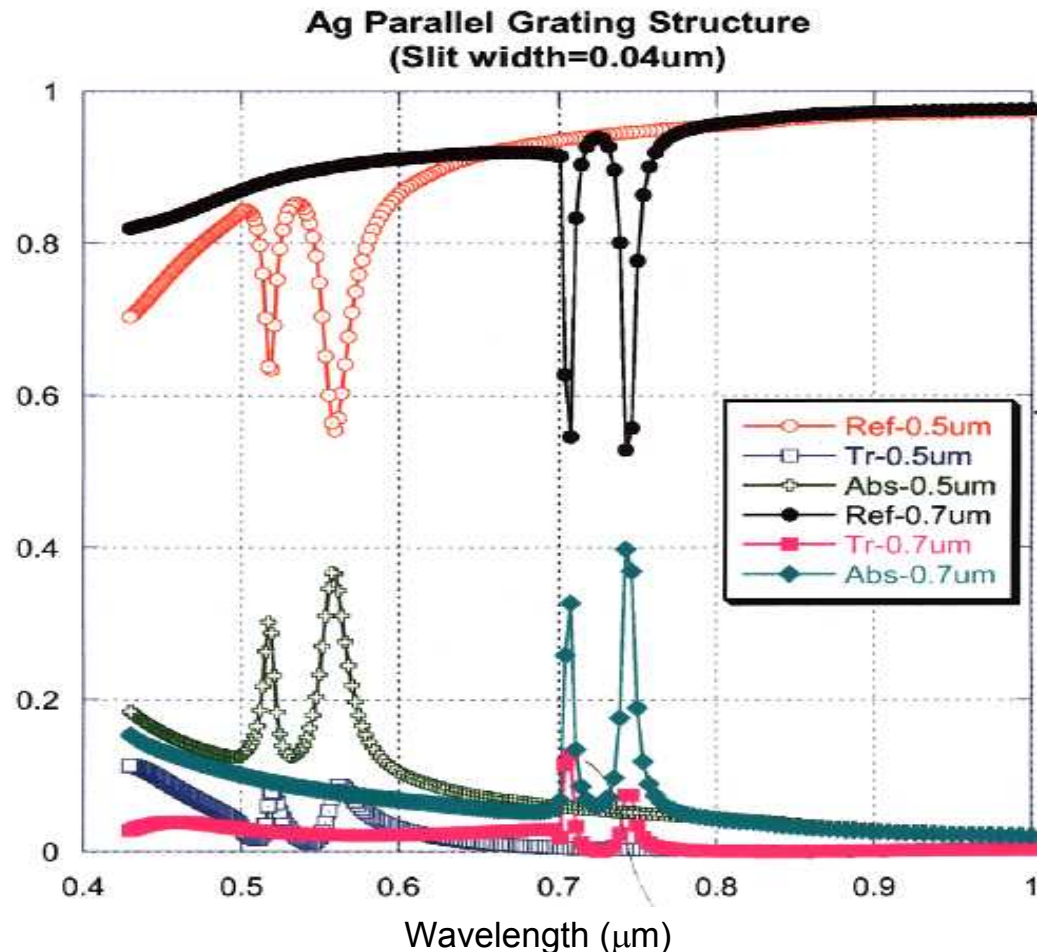


Transmission of $4\mu\text{m}$ wide Gaussian through slit in linearly-patterned silver 300nm thick film with dual-sided 60nm-deep gratings.

Emissivity calculated using transfer matrix method

Demonstrates ability to model and design absorption peaks in real metal films.

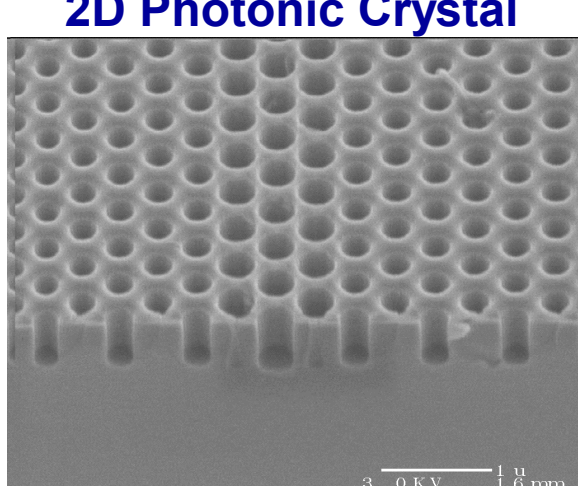
Double peak the result of changes in discretization to decrease run time.



Photonic crystal modeling and fabrication

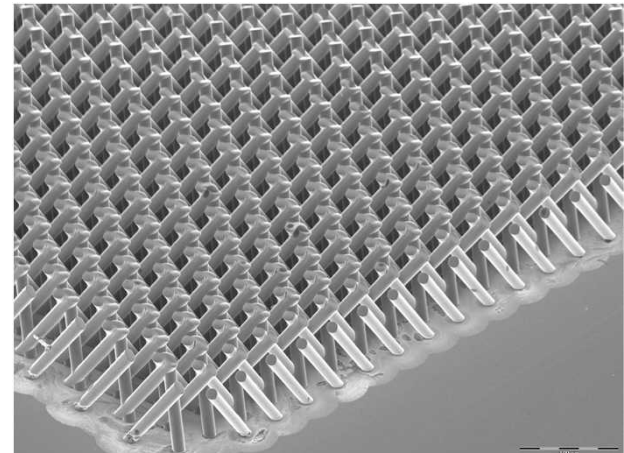
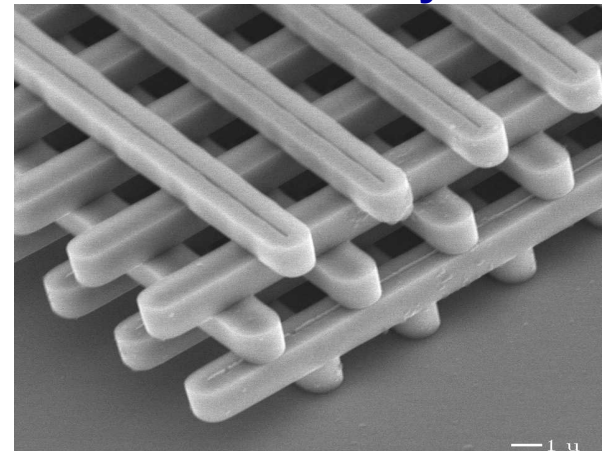
Photonic crystals have a “photonic bandgap” in the same way that semiconductors have an electronic bandgap.

The crystal structure determines the bandwidth and frequencies of the bandgap.



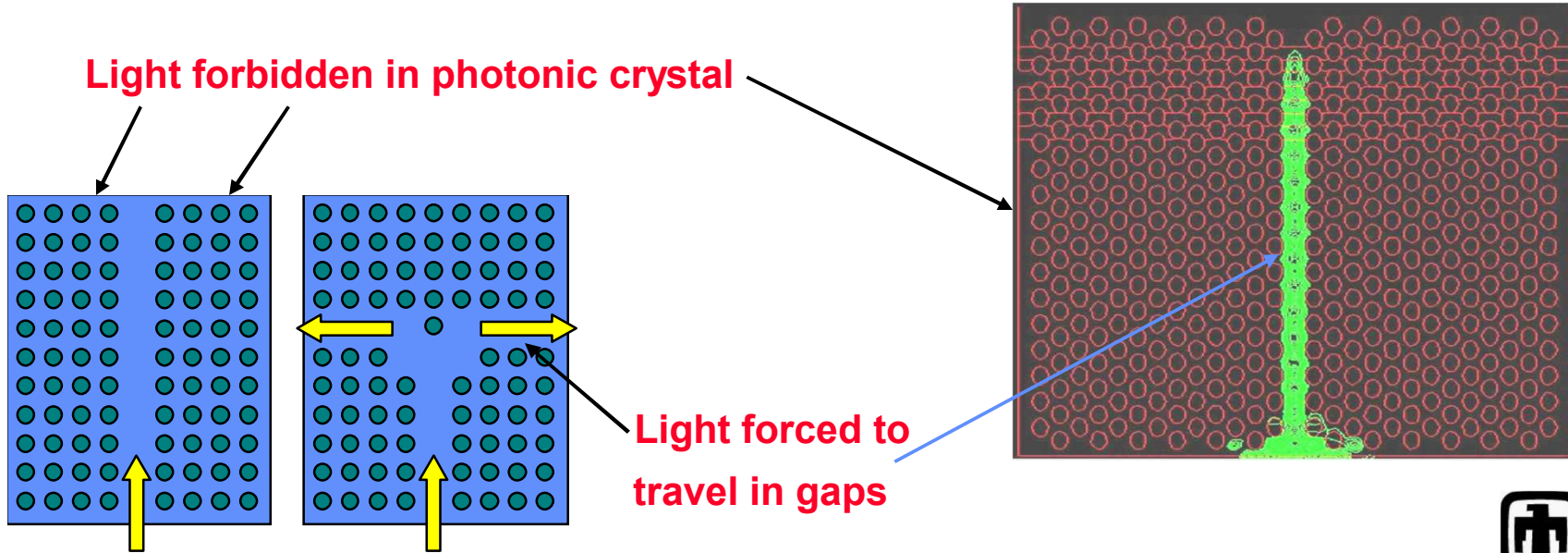
2D Photonic Crystal

3D Photonic Crystals

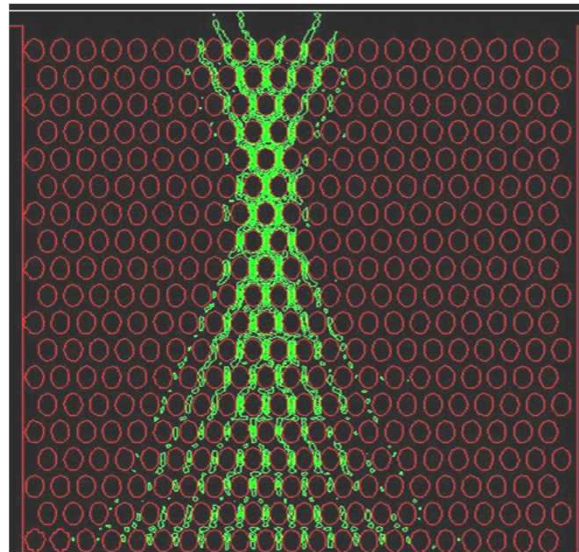


2D photonic crystals

- Light is **forbidden** in areas of the photonic crystal at certain wavelengths.
- We can make sharp bends
- We observe a **negative index of refraction** at some wavelengths
- We observe a “**superprism**” effect at some wavelengths: where a small incident angle change will lead to a huge change in the transmitted angle

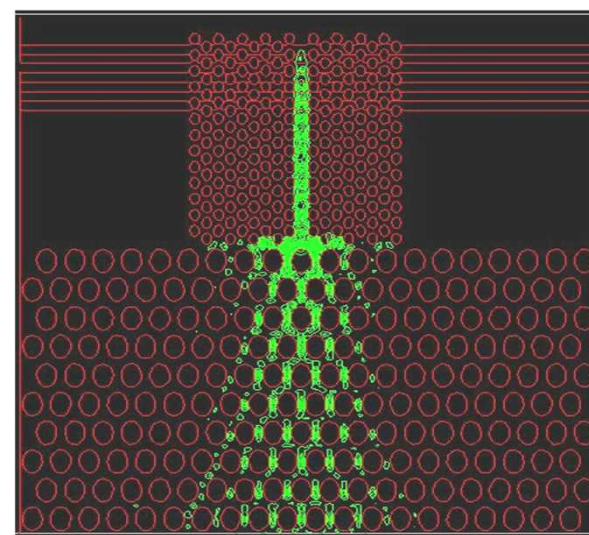


2D photonic crystals

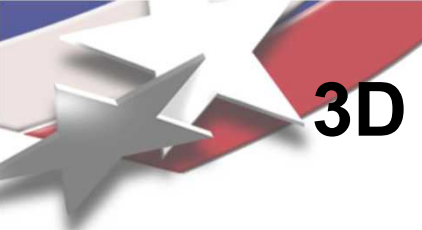


Incident Gaussian diverging beam

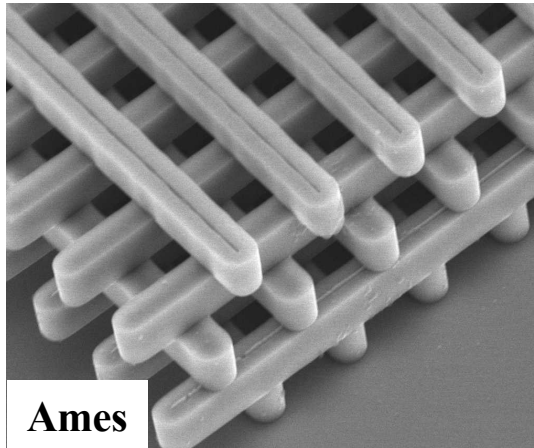
- Photonic crystal can have a **negative index of refraction**
- Causes a diverging beam to converge
- Allows us to **couple** a beam into a photonic crystal waveguide



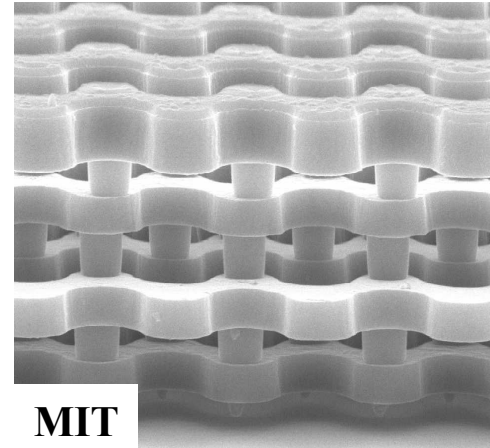
Downside of 2D photonic crystals is a large out-of-plane losses.



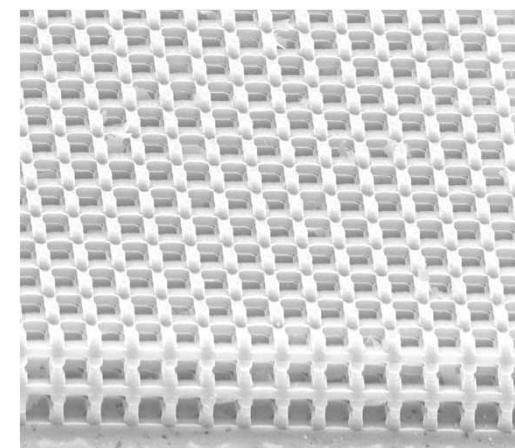
3D photonic crystals using Sandia's silicon advanced processing



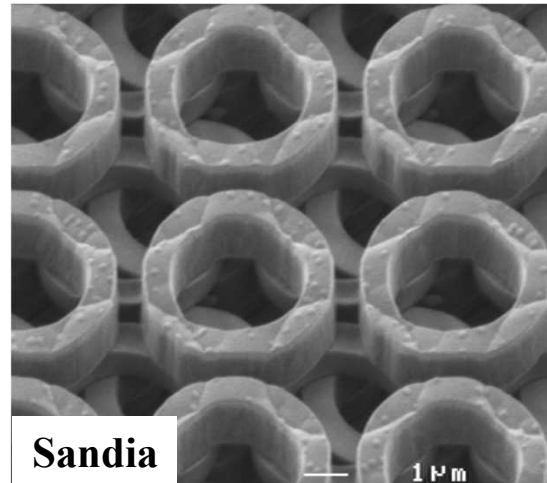
Diamond



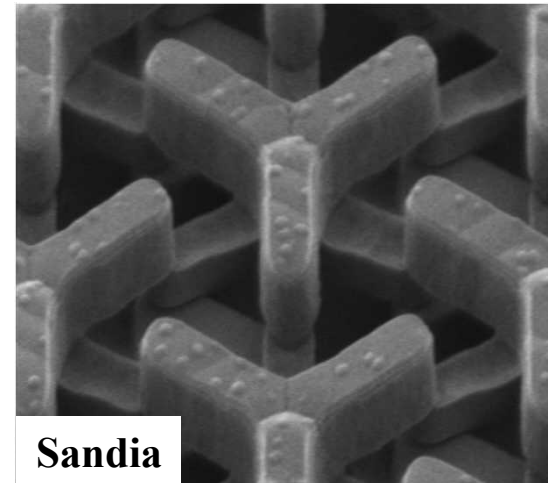
Diamond



Simple Cubic



FCC

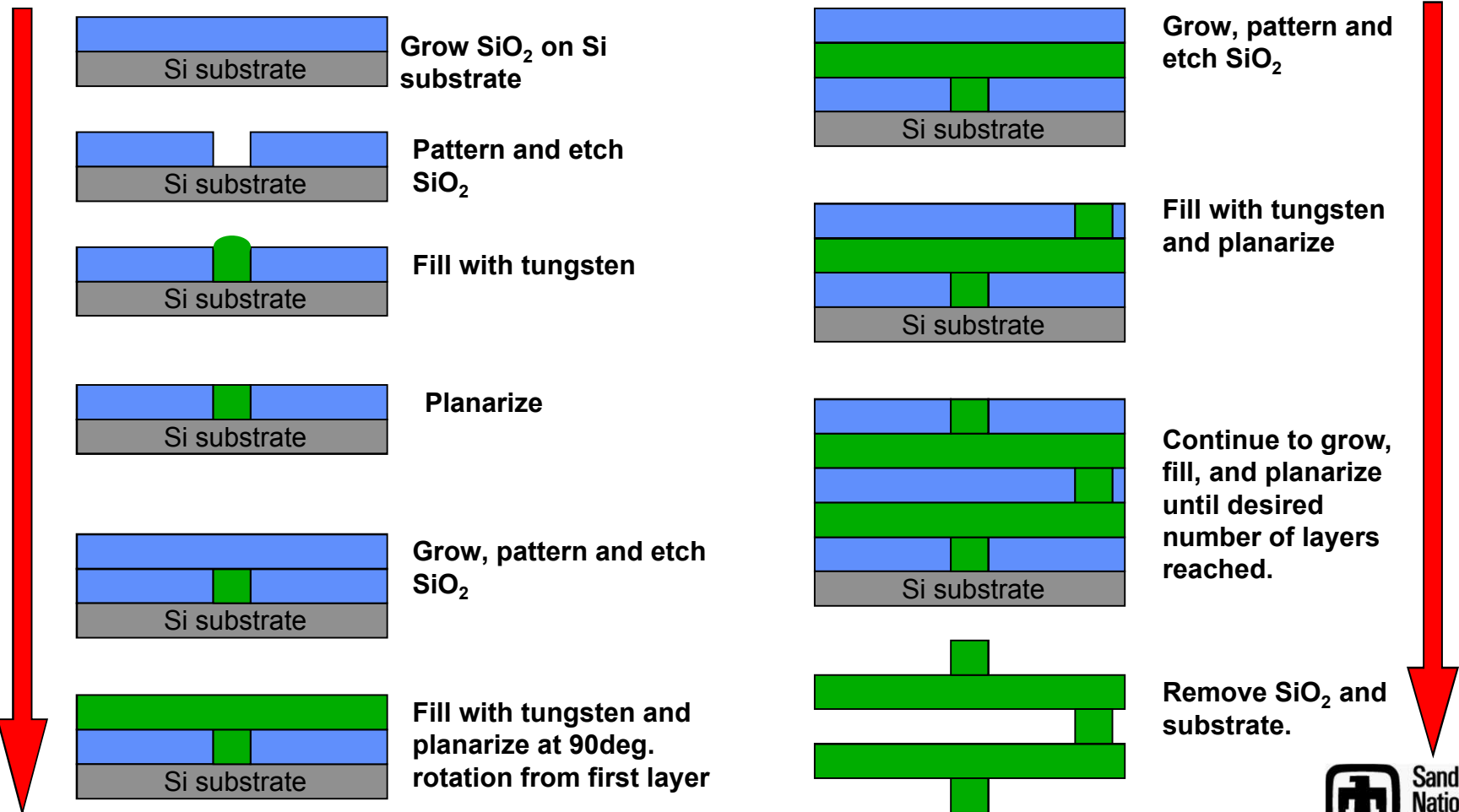


FCC



Logpile fabrication steps

Modern lithography allows optical-frequency photonic crystals.

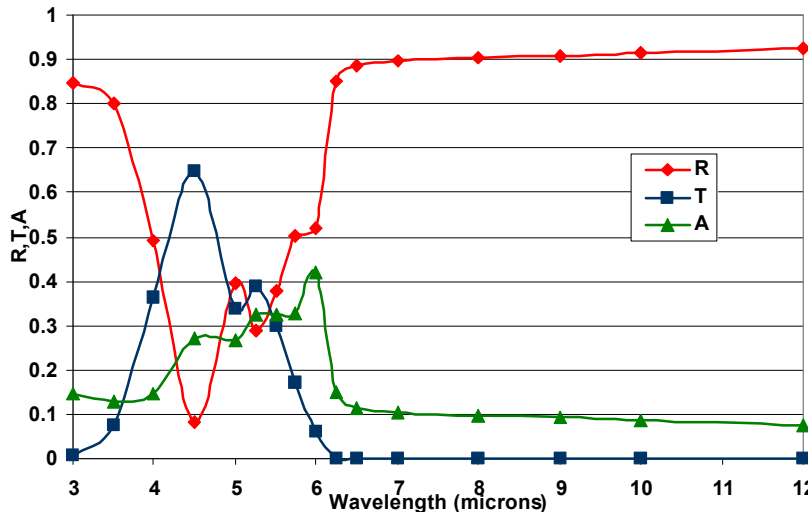


Sandia
National
Laboratories

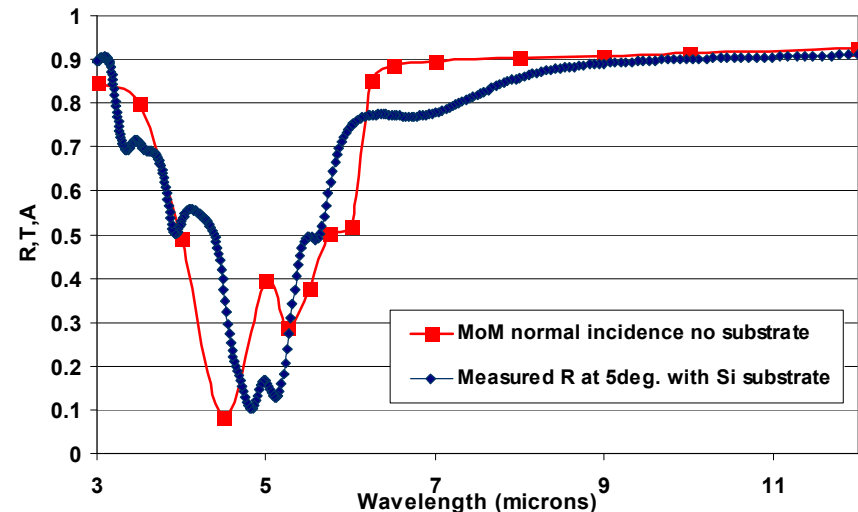
Method-of-moments results for finite conductivity metal

For 8-layer logpile sample with no substrate or fill material.
Uses published value for tungsten conductivity.

MoM results for reflectivity, transmissivity, and calculated absorptivity



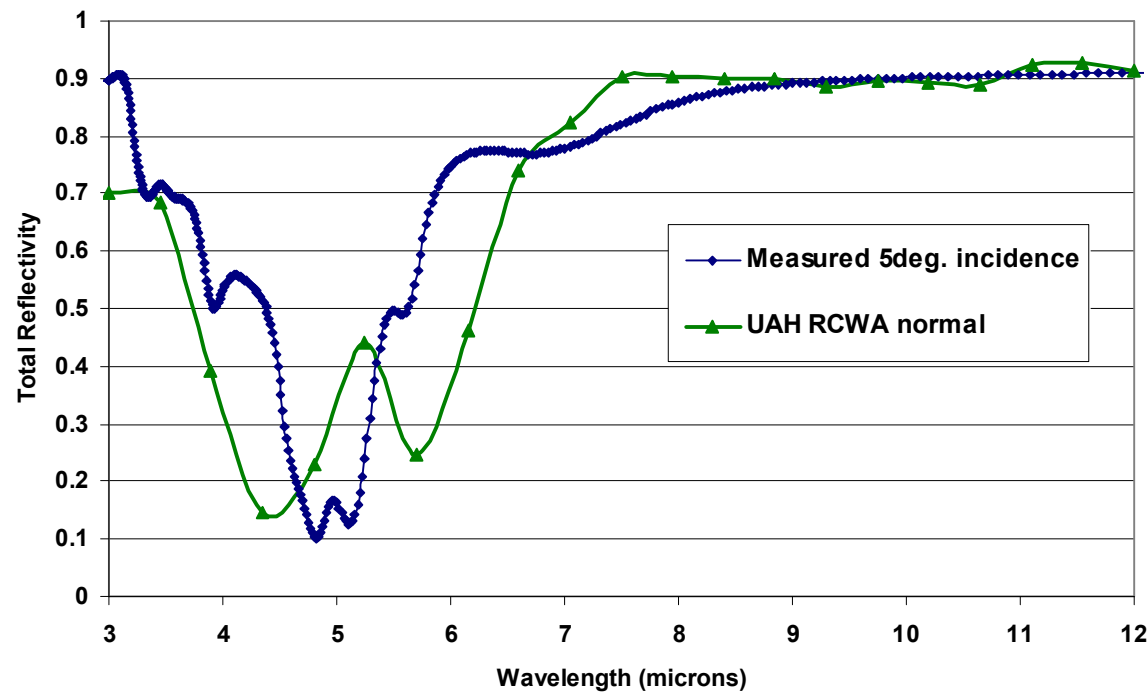
Comparison of MoM reflectivity to measured sample*



* MoM results are normal incidence with no substrate. Measured results are 5° from normal with silicon substrate.

Conductivity of tungsten deposited is slightly lower than published conductivity for bulk tungsten.

Comparison of measured results to UAH RCWA code





Conclusions

- **Sandia has numerical modeling and fabrication capabilities for a broad range of photonic applications.**
- **Modeling takes several forms, using the most applicable tool for the task.**
- **We are always searching for more powerful and efficient modeling tools.**